THE ROTOR SYSTEM AND FLYING QUALITIES OF PERISCOPTERS

THE ROTOR SYSTEM AND FLYING QUALITIES OF PERISCOPTERS

By

SURESH K. GUPTA, M.E.

A Thesis

Submitted to the Faculty of Graduate Studies

in Partial Fulfilment of the Requirements

for the Degree

Master of Engineering

McMaster University

April 1969

MASTER OF ENGINEERING (1969) McMASTER UNIVERSITY
Hamilton, Ontario.

TITLE: The Rotor System and Flying Qualities of Periscopters

AUTHOR: Suresh K. Gupta, B.E. (Delhi University)
M.E. (Indian Institute of Science)

SUPERVISOR: Professor E. O. Gadamer

NUMBER OF PAGES: v, 113

SCOPE AND CONTENTS:

Prototypes of the recently developed periscopter, a flying platform tethered to a ground station, are presently extremely difficult to fly. Tests conducted by the Defence Research Board of Canada in Valcartier, Quebec, and by Westinghouse of Canada near Hamilton, have led to several crashes. Possible causes for the lack of flying qualities are: unbalanced aerodynamic forces and moments; inadequate controls; and poor inherent stability characteristics.

In this investigation, the system of counter-rotating lifting rotors used in the present periscopters is examined with a view to improvement of the flying qualities. The aerodynamic theory of helicopter rotors is considered as a background.

The blades of the present periscopter rotors neither flap nor feather. The feasibility of using either articulated (flapping) blades or rigid feathering blades is examined. It is found that flapping blades are not feasible mainly because of associated stability and

control problems. Also the two counter-rotating rotors would tend to strike against each other. A rigid rotor system featuring feathering blades is found to be feasible. Such a system is therefore examined in detail by computing all relevant aerodynamic parameters. It is shown that the feathering system can provide all required control moments. Its introduction would therefore eliminate the present bail mechanism.

An analysis of the stability characteristics of a periscopter featuring a rigid feathering rotor system is developed. However, when hovering in still air, such a periscopter is shown to be unstable. The possibility of rendering it stable by the use of rotor controls is demonstrated. No attempt is made to suggest a specific design for the control system to be used.

The effect of various operational parameters on the flying qualities of the periscopter is investigated.

ACKNOWLEDGEMENTS

The author expresses his sincere appreciation for the guidance and assistance given by Professor E. O. Gadamer of McMaster University. The author expresses his thanks to Mr. R. S. Mitchell and Mr. C. J. Wilson of Canadian Armament Research and Development Establishment for their help and suggestions.

Financial assistance received through Defense Research Board grant number 9540-09 is gratefully acknowledged.

TABLE OF CONTENTS

1. INTRODUCTION

Periscopter is the trade name of an unmanned flying platform tethered to a ground vehicle. The platform is kept aloft by two electrically driven counter-rotating rotors (propellors). The periscopter is jointly developed by the Defence Research Board of Canada and by Westinghouse of Canada. The system is designed to accommodate a television camera that can overlook a limited ground area of military or other interest from a height of up to 600 feet.

Several periscopter prototypes have been built and tested in recent years. Some have crashed. None has as yet performed to the full satisfaction of the research and development teams, and no commercial production has so far been contemplated. The purpose of this research is to investigate the aerodynamics and dynamics of the periscopter types now in existence, and to gain some understanding through theoretical analysis of the causes for the crashes. Suggestions are made for design changes. A simultaneous investigation of an advanced test program for the periscopter is in progress at McMaster University.

The tether cable of the periscopter system connects the flying platform to a ground vehicle. The design of the cable consitutes a formidable engineering problem. The cable must perform three functions. It must hold the platform in the air much like the string of a kite prevents the kite from escaping. Therefore the cable must be light and strong. Its tension is the aerodynamic lift minus the weight of

the platform. The cable must contain electrical leads of sufficiently good conductivity and insulation for powering two electric motors developing each up to five horsepower Finally, the cable must contain additional electrical leads to serve both the control system and the electronic devices (television camera) of the platform. Research toward development of a better cable is necessary but has not been included as part of this investigation.

The flying platform and the tether cable have a combined weight of the order of 100 pounds. The required aerodynamic lift is generated by a system of two coaxial counter-rotating rotors approximately four feet in diameter. In still air the rotors move in two horizontal planes whose design distance is approximately three inches apart. The rotor blades are made of light rigid material. There occurs, nevertheless, some in-flight blade flexing. This flexing is currently held responsible for the collisions that have occurred between the two rotors and that have caused the crashes during test flights.

A simple platform lifted by two counter-rotating rotors is capable only of hovering in still air. If there is an incident wind of constant velocity, or if there are random gusts, the simple tethered hovercraft becomes completely unstable and will crash. Control devices are therefore used to render the periscopter aerodynamically and dynamically stable within a wide range of wind conditions. The

following control moments are essential: A yaw moment must be available for the case when the reactions of the counter-rotating propellors do not fully compensate. This condition occurs when there is non-zero wind velocity resulting in non-identical upstream flows for the two rotors. A pitch moment and a roll moment must be available when, because of winds or gusts, the rotors develop unbalanced pitch and roll. These moments also serve to manoeuver the platform within the constraints of the tether cable.

In the existing periscopter models control moment for yaw is generated by increasing or decreasing the speed of one rotor with respect to the other rotor. This changes the net reaction torque which must be zero. The control mechanism consists of a sensing device that controls the speed of the two electric generators in the ground vehicle supplying the power for the rotor motors. (The motors are of the induction type so that their speed changes with the frequency of the electric power and therefore on the generator's rpm.) The yaw control is thus fully automatic. It involves considerable ground equipment.

The control moments in pitch and roll are presently generated by torquing the platform against a bail mechanism. In the latest periscopter prototype, Skyhook IV, at the Canadian Armaments Research and Development Establishment (CARDE) the bail is six feet long and carries at its lower end a weight of about four pounds. The upper end of the bail is hinged near the centre of gravity of the periscopter. Torquing is produced by two direct current servo motors,

one for pitch and one for roll. The torquing motion of the bail is constrained by the tether cable whose tension is in the order of thirty pounds. Because of this tension the bail deflections are very small.

2. HELICOPTER DYNAMICS AND AERODYNAMICS

To our knowledge, no analysis of periscopter type aircraft has as yet been published. Our analysis of the aerodynamics of the periscopter rotors is an extension of the known aerodynamics of the helicopter rotor. For this reason, some relevant facts of the dynamics and aerodynamics of helicopter rotors are reviewed in this section. We specifically mention single-rotor aerodynamics and the calculation of a rotor induced velocity field. Rotor types used in modern helicopter designs are discussed.

SYMBOLS USED

r	radius of the rotor
b	number of blades
c	blade elemental chord
x	non-dimensional radius r/R
Ω	rotational speed of the rotor (radians/second)
Ψ	blade azimuthal angle measured from downwind position
v_i	induced velocity
V	wind velocity
V'	resultant velocity at the blade element
U_T	velocity component in the plane of the rotor
U_P	velocity component perpendicular to the plane of the rotor
V_c	climb velocity
α	rotor disc incidence
θ_c	collective pitch setting

ϕ downwash angle (U_T/U_P)

i blade elemental angle of attack

μ tip speed ratio ($U_T/\Omega R$)

λ $U_P/\Omega R$ inflow ratio

λ_{ol} $v_i/\Omega R$

K factor for longitudnal variation of induced velocity

ρ air density

T thrust

H H-force

Y Y-force

p disc loading ($T/\pi R^2$)

2.1 Rotor Aerodynamics

No complete analysis exists for the aerodynamics of helicopters rotors. The flows encountered, especially in forward flight, are very complex. They are non-linear and unsteady (time-periodic). Consequently, a manageable analysis must rest on some simplifying assumptions.

Figure 1 (see Appendix 1) shows the effects of a hovering rotor in still air. A pressure difference Δp develops across the plane of the rotor. The pressure difference causes the air above the rotor to accelerate and to pass through this plane. The induced velocity v_i, also called the rotor downwash, is defined as the velocity of the air when passing through the rotor plane. Downstream of the rotor plane the air is further accelerated until it reaches a distance

of about one rotor diameter. In forward flight, this distance reduces to as much as one rotor radius.

The forces and moments acting on the helicopter rotor blade can be investigated by analyzing the flow past a rotor blade. Figure 2 shows the top view of a blade that rotates counter-clockwise. R and Ψ are respectively the rotor radius (blade span) and the time-dependent azimuthal angle of the rotating blade. Ω is the angular speed. Figure 3 shows the elemental section of the blade at a typical distance r from the center. As the blade rotates, the elemental section moves through the air with velocity Ωr. Ωr is the component of the incident flow velocity vector that lies in the plane of the rotor. The component perpendicular to this plane is the induced velocity v_i. The resultant velocity is denoted by V'. The angle between the direction of the resultant velocity and the direction of the chord of the blade element is the angle of attack i. The angle of attack is the difference between the angles θ_c and ϕ, where θ_c is the angle between the chord and the rotor plane and ϕ is the angle between the flow velocity vector and the rotor plane. One therefore has, since ϕ is small,

$$i = \theta_c - \phi = \theta_c - \frac{U_P}{U_T} \qquad (2.1.1)$$

Considering now the helicopter in motion, one defines three planes for the purpose of introducing a suitable coordinate system. These are the rotor plane, the longitudinal plane, and the lateral plane. The origin is at the rotor center. The rotor plane is already well defined. The z-direction is chosen to be perpendicular to the

rotor plane. The longitudinal plane is then defined by the z-direction and the direction of the flight velocity V. The x-direction is chosen to be perpendicular to the z-direction and in the longitudinal plane. The y-direction is perpendicular to the longitudinal plane. Thus, the xy-plane is the rotor plane, the xz-plane is the longitudinal plane, and the yz-plane is the lateral plane. The aerodynamic force vector (rotor force) in general does not coincide with any of the three coordinate directions. One therefore has the x-component of the rotor force which is usually termed the H-force, the y-component of the rotor force which is termed the Y-force, and the z-component of the rotor force which is identified with the rotor thrust. The thrust is to be distinguished from the lift: if a fourth plane is defined by the directions of the flight velocity and the rotor force, then, by definition, the lift lies in that plane and is the component of the rotor force perpendicular to the flight direction; the drag is defined as the component of the rotor force parallel to the flight direction.

The blade loading is a function of the blade span variable r and the azimuth angle Ψ. The total aerodynamic force developed by a blade for a given Ψ is therefore calculated by integration with respect to r. Since Ψ is a function of time, the time average of the aerodynamic force developed by the rotor is then found by integration with respect to Ψ from 0 to 2π.

The thrust produced by a rotating blade generates a moment about an axis in the rotor plane. This axis is perpendicular to the

blade span, passes through the rotor hub, and rotates with speed Ω. If at a given azimuth angle Ψ the thrust loadings of each blade of a two-blade rotor are identical, the two moments will exactly cancel. In that case the resultant moment at the rotor hub is zero. This ideal condition prevails only if the helicopter hovers in still air. The thrust, and therefore the moment, due to an elemental section of the blade, actually depends on the angle of attack i and on the magnitude of the resultant flow velocity V'. These quantities in turn depend on the induced velocity v_i, which in general is not uniform throughout the rotor plane.

If the helicopter is in forward flight, then the advancing blade ($\Psi = 0^\circ$ to 180°) experiences an increased resultant air flow velocity and an increased angle of attack, c.f. Fig. 3. This increases the thrust loading on the advancing blade. On the retreating blade ($\Psi = 180^\circ$ to 360°) the thrust is decreased. Consequently, the moments are no longer balanced. The resultant unbalanced moment at the rotor hub is largely a roll moment (about the x-axis). Unless neutralized, this moment causes the helicopter to roll over. There is also a pitch moment (about the y-axis due to a variation of the induced velocity in the longitudinal plane), An additional pitch moment may be caused by blade flexing. Again, the helicopter will pitch over unless the pitch moment is neutralized.

2.2 Induced Velocity

The calculation of the distribution of the induced velocity in

the plane of the rotor (rotor disc) is difficult, especially in forward flight. Its determination is nevertheless essential for an analysis of the helicopter's performance, stability, and control. This is because the distribution of the induced velocity determines the distribution of the blade incidence (distribution of the angle of attack along the blade span). The distribution of the blade incidence in turn affects the thrust and the moments, which are the most relevant parameters of the analysis. No accurate theory but approximations based on simplifying assumptions are available.

The calculation of the induced velocity is simple when the helicopter is hovering in still air (Ref. 3, 10, 11). It follows closely well proven propellor theory. Propellor theory is based on the law of conservation of momentum. Despite its simplicity it gives surprisingly good results. The rotor disc with its more or less complicated radial distribution of incidence, loading, etc., is replaced by a thin actuator disc. The actuator disc is assumed to produce a uniform pressure difference across its plane. It thus accelerates the air flow uniformly. In this approximation the induced velocity is calculated as

$$v_i = \frac{T}{2\rho\pi R^2} = \frac{p}{2\rho} \qquad (2.2.1)$$

This expression is of course independent of the blade span variable $x = \frac{r}{R}$.

A more accurate calculation of the induced velocity takes the dependence on the spanwise load distribution into account. The calculation is based on conservation of momentum at a blade elemental section. Its result is the more complicated expression

$$v_i = \left(\frac{V_c}{2} + \frac{\sigma_x a \Omega R}{16} \right) + \left(-1 + \sqrt{1 + \frac{2(\theta_c x \Omega R - V_c)}{\left(\frac{4V_c}{\sigma_x a \Omega R} + V_c + \frac{\sigma_x a \Omega R}{16} \right)}} \right) \quad (2.2.2)$$

Equation 2.2.2 is a function of the span variable x and is very accurate for hovering in still air. It can also be derived by more sophisticated vortex theories. Equation 2.2.2 gives a constant value for the induced velocity over the blade span if σ_x and $\theta_c x$ are independent of the blade span variable x. This implies that the blades are untapered and linearly twisted. For such twist and taper one can therefore use the simple momentum theory (Reference 10).

Considering now forward flight, an approximation of the induced velocity that is uniform over the rotor disc is given by Glauert's formula

$$v_i = \frac{T}{2\rho V' A} \quad (2.2.3)$$

Here V' is the assumed uniform resultant velocity of the air flow through the disc. Equation 2.2.3 is justified only in that it reduces to the momentum equation 2.2.1 when $V' = v_i$, which is the hovering condition. (It also reduces to the expression one finds for the induced velocity of an elliptically loaded wing with the same total

lift and the same span, when V' is taken as the flight speed V.) Glauert's formula is largely empirical. It is regarded in the helicopter literature as a realistic estimate of the mean induced velocity for any forward flight condition (Ref. 3, 11, 20).

In a more refined analysis of the induced velocity in forward flight it is necessary to take the spanwise and the azimuthwise variation into account. The induced velocity is after all a function of the local blade loading. It also depends on the forward speed and on the disc incidence. The fact that the induced velocity depends on both the blade span variable and the azimuth angle affects the aerodynamic characteristics of the rotor. Several theories are available.

One approach takes the longitudinal variation of the induced velocity across the rotor disc into account. As the air is accelerated toward the rotor disc, air particles entering the upstream portion of the disc have experienced the influence of the rotor for less time than air particles entering the downstream portion of the rotor. As a result, the deflection of the air particles toward the rotor increases from the upstream portion to the downstream portion. Thus the induced velocity, being the velocity component perpendicular to the disc, also increases from the upstream portion to the downstream portion. This generates a nose up pitch moment. The effect actually becomes negligible at high flight speeds, say above 60 mph, and is therefore usually ignored in performance and stability calculations. In 1926 Glauert suggested that the increase of the induced velocity in the longitudinal plane is linear. He proposed the

formula

$$v_i = v_o(1 + Kx \cos\Psi) \qquad (2.2.4)$$

where v_o is the mean induced velocity given by equation 2.2.3. The calculation of K is difficult. One approach is to determine independently the distribution of v_i in the longitudinal plane K is then adjusted so that Equation 2.2.4 best fits these data. A theoretical calculation of v_i in the longitudinal plane for a rotor that is uniformly loaded was given by Castles and deLeeuw (Ref. 2). Based on their calculations, K is approximated by the relationship

$$K = \frac{4}{3}\frac{\mu}{\lambda}/(1.2 + \frac{\mu}{\lambda}) \qquad (2.2.5)$$

The tip speed and inflow ratios μ and λ are defined in the table of symbols. Payne points out that the value of K calculated from Equation 2.2.5 agrees better with experimental results than values of K calculated by other methods (Ref. 20).

Mangler in 1953 published an analysis of the distribution of the induced velocity in the rotor plane, based on linearization of Euler's equation of motion. He thus assumed that everywhere in the rotor plane the induced velocity is small compared with the flight velocity. He expanded v_i in terms of a Fourier series in the azimuth angle Ψ. The advantage of Mangler's approach is that it relaxes the assumption that the load distribution is uniform; it thus permits the calculation of v_i to be based on a more realistic load distribution (Ref. 16). It is shown later, however, that Mangler's approach cannot be applied to the rotors of the periscopter because there the induced velocity is of

the same order of magnitude as the wind velocity.

A very accurate though involved method for the calculation of the induced velocity in the plane of a rotor consists of replacing the rotor wake by a suitably chosen vortex system. This method has received increased attention in recent years (Ref. 3, 5, 26, 27). Much computational work is involved. The vortex method is useful in the calculation of the time variation of the induced velocity. Such studies are necessary if one wishes to analyze vibrations or flutter, or for a general aeroelastic analysis. Vortex theories are not used for regular performance and stability calculations.

2.3 Rotor Types

Broadly, there are two helicopter rotor types. These are the flapping rotor, also called the fully articulated rotor; and the cyclic-pitch rigid rotor, whose blades are capable of feathering.

The Flapping Rotor

Each blade of a flapping rotor is hinged near the hub axis so that it can freely flap up and down (Fig. 4). A second set of hinges allows the blades to move through a small angle in the plane of the rotor. Thus the design of the flapping rotor provides one flapping hinge and one so-called drag hinge for each blade. By this design no moments (except a negligibly small blade pitch moment) can be transferred through the hub to the helicopter. Figure 5 shows a flapping rotor. AA is the initial rotor plane. The blades OC and OC' are

flapped up through the flapping angle β. Each blade experiences three forces: the thrust which is nearly perpendicular to the blade span; a centrifugal force which at all times is perpendicular to the rotor shaft; and an inertia force.

The flapping angle β varies as the rotor rotates and is a function of the azimuth angle Ψ. β is determined by the dynamic balance of the three forces and can be approximated by a three-term Fourier series in Ψ. A discussion of the dynamics of flapping blades is given in Ref. 10. Thus

$$\beta = a_o - a_1 \operatorname{Cos}\Psi - b_1 \operatorname{Sin}\Psi \qquad (2.3.1)$$

Because of the negative signs in Equation 2.3.1 the Fourier constants, which are termed flapping coefficients, all become positive. The a_1 -flapping produces a backward tilt of the rotor tip path plane; it is due to the aerodynamic forces that are sine functions of Ψ. a_1 is independent of aerodynamic damping and of the mass of the blade. The b_1 -flapping produces a starboard tilt of the rotor tip path plane if the rotor, as seen from above, moves counter-clockwise; it is due to aerodynamic forces that are cosine functions of Ψ. In Section 4.1 it is shown that b_1 depends on the coning angle a_o and on the longitudinal variation of the induced velocity. When the helicopter hovers in still air, both a_1 and b_1 are zero, and the blades then have a constant flapping angle which is the coning angle a_o.

Flapping of helicopter blades for the purpose of eliminating aerodynamic moments about the rotor hub was first introduced in 1919

by Juan de Cierva (Ref. 7). The flapping motion of the rotating blades in early helicopter models resulted in large periodic in-plane Coriolis forces. Drag hinges were introduced to reduce the resulting periodic in-plane stresses in the blades. Despite this precaution helicopters still crashed. It was found that the presence of the drag hinges led to what is termed ground resonance, an unstable oscillation of the blades about the drag hinges. The problem was eventually solved by the introduction of in-plane damping. Nevertheless, the centrifugal forces experienced by each blade must be borne by sturdy flapping pins which render the rotor hub heavy and of complicated design. Thus, the heavy hub, the in-plane hinges, and the in-plane dampers, all contribute to a structurally complicated design of the flapping rotor. Such helicopters are controlled by tilting the hub, which results in tilting the thrust vector. Their stability and flying qualities are poor and they are structurally complicated. It is possible, however, to improve the stability and flying qualities by moving the flapping hinges away from the hub through a certain fraction of the blade span. Such rotors are termed offset hinge rotors. Many helicopter types currently in use are of the offset type. (For a detailed discussion of offset type rotors see Ref. 19 and 20.)

The Rigid Rotor

Only recently have designs featuring a rigid rotor been given serious attention (Ref. 6, 7, 14). So-called cyclic pitch, or feathering, of the rotor blades is employed to relieve the unbalanced moments produced in forward flight. The blade angle of attack is

varied in a controlled mode by varying the geometric pitch setting as a function of the azimuth angle Ψ. This is made possible by the use of a swash plate mechanism (Fig. 6). The geometric pitch setting as a function of Ψ is

$$\theta = \theta_c - A \cos\Psi - B \sin\Psi \qquad (2.3.2)$$

where θ_c is termed the collective pitch setting. θ_c can be varied during flight. A and B are the feathering coefficients; they may be positive or negative. A forward tilt of the swash plate results in a negative value for the feathering coefficient A, producing a nose-down pitch moment. Similarly, a backward tilt of the swash plate produces a nose-up pitch moment. Roll moments are produced by tilting the swash plate to the right or left. This varies the feathering coefficient B. The collective pitch setting θ_c can be increased or decreased by respectively raising or lowering the entire swash plate.

Helicopters of the rigid rotor design are easily controlled by varying their collective and cyclic pitch. The stability and control characteristics of the rigid rotor helicopter are different from those of flapping rotor helicopters. The more recently developed rigid rotor helicopters have definite advantages over the flapping rotor types. They have a better stability, can be manoeauvered more easily, have a wide center of gravity range, are easy to fly, can be flown by instruments, have high maximum speeds, and are altogether mechanically simpler.

Distinguishing Features of the Periscopter

When analyzing the periscopter for performance, control and stability, it is necessary to clearly bear in mind those features of the periscopter that distinguish it from the helicopter. These are:

(1) The periscopter is tethered to the ground by a cable restricting its freedom of motion. The cable's tension constitutes an additional force that does not exist for the helicopter. The limited freedom of motion and the cable tension may significantly affect the periscopter's stability and control. Helicopter stability and control theory can for this reason not be directly applied.

(2) The aerodynamic efficiency of the periscopter is of secondary importance. Instead, flying qualities must be given first priority.

(3) The close coexistence of counter-rotating blades complicates the aerodynamics. Ineteference affects cannot be taken fully into theoretical account.

(4) Flexing, flapping, and feathering, of counter-rotating blades, pose formidable mechanical design problems.

(5) The periscopter has no forward flight. Nevertheless, flying in a steady wind is aerodynamically equivalent to the forward flight condition of the helicopter.

3. STATEMENT OF THE PROBLEM

The design of the periscopter is complicated. This is because the aerodynamic characteristics of the counter-rotating rotors, the characteristics of the control system, and the stability characteristics, are strongly interrelated. The flying qualities of the periscopter depend on these characteristics. Their improvement amounts to an optimisation of these three factors. For example, the rotor system should be optimised to develop the required lift with a minimum of power. This however becomes a minor consideration. The major concern is the improvement of the flying qualities. There are significant unbalanced forces and moments that depend on the rotor aerodynamics. The control system must balance these forces and moments. Its design must therefore take the rotor aerodynamics into account. Furthermore, in a rigid rotor design employing cyclic pitch the rotor itself would provide the control. The design of the control system must also take the periscopter's stability characteristics into account. The stability characteristics in turn depend among other things on the rotor aerodynamics.

It follows that the investigation of the periscopter must follow a course that begins with the aerodynamics of the rotor system, followed by an understanding of the control and stability problem. This leads to a theoretical prediction of attainable flying qualities.

The periscopter rotor systems employed in current designs do

not feature blade flapping or feathering. These systems have caused considerable trouble (including the crashes) when flight-tested. The upper and lower blades tend to flex and strike against each other. The effect must be studied in terms of the rotor aerodynamics. The periscopter flying qualities have been very unsatisfactory at wind speeds as low as 10 feet per second. At speeds in the order of 20 feet per second it is almost impossible to fly the present models. It is clear that the control and stability characteristics of the present models are inadequate in relation to their aerodynamics.

The feasibility of replacing the periscopter's present simple system of rotors by more elaborate alternative systems is examined. Blade flapping and feathering are specifically investigated. Since one is ultimately interested in the flying qualities of the periscopter, a combination analysis of the aerodynamics of the rotor system, the control system, and the stability, is carried out. It is shown that the introduction of blade flapping is not feasible, but that the introduction of blade feathering promises a significant improvement of the flying qualities.

3.1 The Flapping Rotor

In the case of a flapping rotor system, no aerodynamic moments produced by the rotor would be transferred through the hub to the periscopter. Nevertheless, the incident wind would cause the rotor tip path plane to tilt backward and sideways. This is because of the existence of the a_1-flapping and the b_1-flapping discussed in

Section 2.2. The tilt of the rotor tip path plane causes a tilt of the thrust vector. This means that the thrust vector no longer passes through the center of gravity of the periscopter. Moments would therefore be created about the center of gravity, and the control problem would thus still exist. Control could be achieved in two ways. One could use a bail mechanism. The present bail mechanism would have to be redesigned because the performance of the systems used in current periscopter models has not been found satisfactory in flight tests. Alternatively, the hub could be tilted. This would result in a tilt of the rotor tip path plane. Tilting of the hub is accompanied by mechanical difficulties. This is true for helicopters, and would be even more severe for the counter-rotating system of the periscopter with its two distinct tip path planes.

Flapping blades would create another serious problem. The b_1-flapping would cause one rotor to tilt in one rolling direction and the other rotor to tilt in the other rolling direction. This means that on one side the rotor blades would come much closer together than is provided for by the design distance of the two rotor planes. Therefore they would tend to strike against each other.

Some calculations of b_1-flapping have been made. They show that the b_1-flapping of each rotor can be as large as six degrees, giving each blade a tip deflection of about three inches. To this must be added an allowance for possible vibrations or flutter of the blades. Thus, in order that the perilous interference of the two rotors be completely eliminated, their present distance of three

inches would have to be considerably increased, say to eight inches. Eight inches would not be a small distance compared with the rotor diameter.

Moving the rotor discs apart to a relative distance that is comparable, or almost comparable, to the disc diameter would complicate the aerodynamics of the system. Theoretical analysis of such a configuration seems impossible. It should of course be feasible to conduct wind tunnel tests.

In a configuration featuring a safe distance between the two rotors, the air flow occupying the space between the two rotors would be accelerated under the influence of both rotors. This would result in a higher induced velocity at the lower rotor so that the difference in the induced velocity at the two rotors could no longer be neglected. The inflow conditions at the lower rotor would be influenced by the skew angle of the wake of the upper rotor, and also by the wake's interaction with the incident wind. It would thus be imperative to employ a different design for each rotor. The design of each rotor would have to be based on the aerodynamic effect, to be determined experimentally, of the distance between the two rotors.

The b_1-flapping depends on the coning angle a_o and on the longitudinal distribution of the induced velocity. The coning angle could be kept small by the use of heavy material for the blades and by choosing a suitable load distribution over the blade span. However, the major cause for the b_1-flapping is the longitudinal variation of

the induced velocity. This effect cannot be eliminated through design. For high wind speeds, however, the slip stream is almost horizontal, and the longitudinal asymmetry of the induced velocity is negligible. But for the transition range of wind speeds (10 to 50 feet per second), the induced velocity decreases as the wind speed increases, and the longitudinal asymmetry of the induced velocity increases. This results in increased b_1-flapping.

A flapping rotor design would involve significant mechanical problems. There would have to be a heavy hub to accommodate each rotor's flapping pins, in-plane hinges, and the in-plane dampers, (see also Section 2.3).

Finally, flapping rotors have very poor stability characteristics (Ref. 10). Despite the design possibilities mentioned, it is therefore unlikely that the introduction of flapping rotor blades would improve the periscopter's flying qualities.

It follows from this discussion that the adoption of a flapping rotor system for the periscopter is not promising. For similar reasons one should also reject the adoption of off-set flapping hinge rotors, sea-saw rotors, and stiff-hinged flapping rotors.

3.2 The Rigid Rotor

It was said in Section 2.3 that the unbalanced moments experienced by the periscopter and caused by winds and gusts could be effectively neutralized if the blades were given a suitably chosen

cyclic pitch (feathering) as they rotate in azimuth. Not only could the aerodynamic moments in this way be neutralized, but any desired control moments could be produced by the use of cyclic pitch. Bail mechanisms could therefore be completely eliminated. It should also be possible to use the collective pitch for yaw control. This would result in the elimination of some of the ground equipment currently needed for yaw control.

The history of the rigid rotor with feathering blades began as recently as 1957. At that time the Lockheed Company encouraged a research and development group consisting of non-conformist aerodynamicists to investigate the design feasibility of an air vehicle that could take off and land vertically, should be relatively quiet, should have low downwash velocity, and could be mass produced. Helicopters were found to be the answer. But at that time helicopters were very complicated in design and had poor flying qualities. Flapping blades were still used. The Lockheed group began to search for a new helicopter concept featuring both a simpler mechanical design and more satisfactory flying qualities. The principal problem was to find improved means for producing control moments. The concept of a rotor, whose blades do not flap but whose incidence changes as a function of azimuth, was adopted as a result of the research. Such rotors are the now known rigid feathering rotors. Lockheed thus revived a concept that had been abandoned as impractical during the early years of the helicopter. The promise shown by the rigid rotor concept - with its potential for hands-off stability - led to an extensive development program. The advantages of the rigid rotor helicopter were found to

be a much simpler mechanical design, improved inherent stability, and better control and manoeuverability (Ref. 13). The improvement in stability is accomplished by a control gyro mounted above the blades. The first two Lockheed 286 helicopters were certified in 1967. They were the first rigid rotor vehicles certified by the Federal Aviation Administration of the United States.

Adoption of the rigid rotor concept for the periscopter appears very promising. Some mechanical problems would of course have to be overcome. Each rotor would have to be feathered by an individual swash plate mechanism.

To establish the suitability of a rigid rotor system for the periscopter, a theoretical analysis of the aerodynamics of counter-rotating rigid rotors with feathering blades, and of the relevant stability and control problem, has been carried out. The analysis is presented in Section 4.

4. THE RIGID ROTOR SYSTEM

A rigid feathering rotor system is investigated. The system consists of two coaxial and counter-rotating rotors. The rotor design of the existing periscopter models is considered. Each rotor has two identical blades which are tapered but not twisted. The diameter of each rotor is 52 inches and their design speed is 3000 rpm. The distance between the two rotor planes is three inches. The total available power is approximately 8.5 horse power, and both rotors produce a total thrust of 95 pounds.

4.1 Aerodynamic Analysis

ADDITIONAL SYMBOLS USED

C_o root chord

c blade elemental chord

t_n taper integral of order n

v_o mean induced velocity

λ_{o1} $v_o/\Omega R$

λ_{o2} $\frac{V \sin \alpha}{\Omega R}$

λ $\lambda_{o1}+\lambda_{o2}$

δ mean drag coefficient for blade section

M mach number

x_2-x_1 effective blade radius

A' effective rotor disc area

Y $\frac{1}{8}\rho a C_o \Omega^2 bR^3$ $(b = 4)$

Y_M $Y R/2$

C_T coefficient of thrust (thrust/Y)

C_{MR} coefficient of roll moment (roll moment/Y_M)

C_{MP} coefficient of pitch moment (pitch moment/Y_M)

C_Q coefficient of torque

In this section, a mathematical model is considered for the computation of the aerodynamic forces and moments developed by two counter-rotating rigid feathering rotors, such as could be employed in a periscopter. Since every mathematical model constitutes a compromise between the complexity of the live configuration it is to describe, and the requirement that the computations be manageable, it is necessary to go through some preliminary speculations as to what effects, if any, can be neglected. Such considerations lead to a set of simplifying assumptions.

To obtain average values, the forces and moments developed by an elemental section of a blade must be integrated over the blade span and over the azimuth angle (see Section 2.1). In order that integration in closed terms be possible, such variables as the chord, the twist, the induced velocity, etc., must be reasonably simple functions of the blade span variable x and of the azimuth angle Ψ. Assumptions are formulated not only for the purpose of simplification but also because of lack of information, for example, assumptions are made about the unexplored aerodynamic interaction between two co-axial rotors, about the induced velocity distribution, and about tip losses.

The assumptions made and their justifications are listed in the following items (1) to (13). Some remarks on computational procedure are also made.

Assumptions

(1) Wind data. A wide range of wind velocities is considered. Computations are made in steps of 10 feet per second from zero (hovering in still air) to 60 feet per second. The wind incidence is varied in steps of ten degrees from -20° to $+20^{\circ}$.

(2) Blade chord taper. In most simplified helicopter analysis the blade chord is assumed to be uniform along the blade span. However, in the present analysis the spanwise variation of the chord is taken into account. The blades are linearly tapered. If c is the chord length of the elemental section at the span station x, then

$$c = C_o(1-t^* x) \tag{4.1.1}$$

where $$t^* = \frac{\text{root chord - tip chord}}{\text{root chord}} .$$

The varying chord is easily taken into consideration by the use of taper integrals which are defined as

$$t_n = 4 \int_{x_1}^{x_2} (1-t^* x)\, x^{n-1}\, dx \tag{4.1.2}$$

where $n = 1, 2, 3 \ldots .$

(3) Blade twist. The periscopter rotor blades have zero twist. Nevertheless, for the sake of generality a linear twist can be introduced into the analysis. Thus

$$\theta_c = \theta_{CR} - \theta_{cr} x \tag{4.1.3}$$

where θ_{cr} is the total twist from root to tip. θ_{cr} is set equal to zero in all computations.

(4) Tip loss factor and effective disc area. Some spillage of air from the lower surface of a blade to its upper surface occurs at each rotor blade tip. This results in a reduced thrust near the tip. The effect is known as the tip loss. Experience shows that the tip loss can be taken into account by introducing an effective blade span (Ref. 10). One thus has the dimensionless effective outer radius of the blade

$$x_2 = (1 - \frac{\text{tip chord}}{2R})$$

for the existing periscopter rotor blades $x_2 = 0.96$.

Because of the existence of a hub and an aerodynamically ineffective blade root, there exists an effective inner radius of the rotor, whose dimensionless value for the present periscopter is $x_1 = 0.15$.

The effective disc area is then

$$A' = \pi R^2 x^2 - \pi R^2 x_1^2$$

$$= \pi R^2 (x_2^2 - x_1^2)$$

$$= \pi R^2 e \quad , \qquad (4.1.4)$$

where $e = 0.92$.

It is important to note that the tip loss factor is relevant

for the calculation of the forces and moments, but is not relevant for the calculation of the power consumed. Thus, for the calculation of the power consumed, x_2 must be set equal to one. One therefore has two taper integrals. One in which $x_2 = 1.0$ and which is used for power calculations , the other in which $x_2 = 0.96$ and which is used for the calculation of all other aerodynamic parameters.

(5) Blade feathering. The rotor blades are allowed to feather. The geometric angle of incidence θ is a function of the azimuthal angle Ψ. Thus

$$\theta = \theta_c - A \cos \Psi - B \sin \Psi \qquad (4.1.5)$$

(6) Induced velocity. There are two co-axial rotors whose planes are three inches apart. Each rotor disc has a diameter of 52 inches. The distance between the discs is therefore about one-seventeenth of the diameter. The air is somewhat accelerated in the region between the rotors. The induced velocity is therefore higher at the lower rotor than it is at the upper rotor. The effect can be expected to be negligible as long as the distance between the rotor planes is small compared with the rotor diameters. This is considered to be the case in the present configuration. For computation purposes, both rotors are therefore assumed to be in the same plane, and the induced velocity is thus calculated as if the system of two two-blade rotors were replaced by a single rotor that has four blades.

Equation 2.2.2 is used for the calculation of the induced velocity distribution in still air. The distribution is shown in Figure 7. However, for further calculations the induced velocity

shown in Figure 7 is replaced by a linear distribution

$$v_i = H + Gx$$

where it is estimated (from Figure 7) that G = 36 feet per second and H = 15 feet per second. With these values,

$$v_i = 36x + 15 \ . \qquad (4.1.6)$$

Equation 4.1.6 is used for the calculation of the thrust developed in still air. The thrust obtained is 96.1 pounds. From this value one can calculate the average induced velocity from simple momentum theory (Equation 2.1.1). One obtains 39.03 feet per second. This is very nearly the value given by Figure 7 for x = 2/3. It is in agreement with the general practice of using the value of v_i given by blade element theory (Equation 2.2.2) for x = 2/3. The value obtained in this way is usually considered as representative of the average induced velocity.

In steady winds, the calculation of the induced velocity is more complicated. The various procedures available were discussed in Section 2.2. Equation 2.2.4 is simple and suitable for present purposes. Thus

$$v_i = v_o(1 + Kx \cos \Psi)$$

where $$K = \frac{4}{3} \frac{\mu/\lambda}{(1.2+\mu/\lambda)}$$ (see Equation 2.2.5).

The lateral variation of the induced velocity over the disc is ignored as the relevant quantity $k = \frac{-16e\mu^3}{a\sigma_R t_4}$ is very small in the present

analysis (Ref. 20).

The average value of the induced velocity v_o over the disc is

$$v_o = \frac{T}{2A\rho eV'} \quad \text{(Glauert's Formula)}.$$

One can also write

$$v_o V' = \frac{T}{2A\rho e} \quad . \tag{4.1.7}$$

Thus v_o is known in terms of the thrust T. But T depends on the dimensionless induced velocity λ_{o1} according to

$$T = Y(\theta_c t_3 + \tfrac{1}{2}\mu^2 t_1 \theta_c - t_2\lambda_{o2} - B\mu t_2 - \lambda_{o1} t_2) \quad \text{(Equation 4.1.12)}$$

which can be rewritten as

$$T = Y(xy - t_2 \lambda_{o1}) \quad . \tag{4.1.8}$$

If Equation 4.1.8 is substituted into Equation 4.1.7, one obtains after division by $(\Omega R)^2$

$$a_1\lambda_{o1}^4 + a_2\lambda_{o1}^3 + a_3\lambda_{o1}^2 + a_4\lambda_{o1} + a_5 = o \tag{4.1.9}$$

where $a_1 = 1.0$

$$a_2 = 2\lambda_{o2}$$

$$a_3 = \lambda_{o2}^2 + \mu^2 - (YYY)t_2^2 \tag{4.1.10}$$

$$a_4 = 2(xy)\,(YYY)t_2$$

$$a_5 = -(YYY)\,(xy)^2$$

and $$(YYY) = \left[\frac{Y}{(2\rho Ae)\,(\Omega R)^2}\right]^2 \quad .$$

Equation 4.1.9 is solved numerically, using Bairstow's method and a digital computer. Computations are carried out for each relevant value of the wind velocity V and the wind incidence α. λ_{ol} is given by the positive real root of Equation 4.1.9. Results are shown in Appendix 1, Table 1. The Fortran IV program for the calculation of λ_{ol} is also presented in Appendix 1.

(7) Flexing of blades. Blades are never perfectly rigid and therefore flex under an aerodynamic load. The effect of flexing can be approximated by introducing a constant coning angle a_o into the analysis. The value of a_o is a function of the blade stiffness. a_o effects only the pitch moment. (The effect on the down wash angle ϕ is negligible.) The relation between the pitch moment and a_o is linear; c.f. Equation 4.1.17. Since a_o is not known for the present periscopter blades, it is set equal to one degree for the purpose of all calculations. This is justified in view of Equation 4.1.17 whose terms not involving a_o turn out to be very predominant.

(8) Lift as a function of incidence. The lift coefficient is assumed to depend linearly on the incidence. The slope of the straight line representing C_L against i is taken to be 6/radian. (The blade section is NACA 0012 for most of the blade span.) This value is adopted for all calculations.

(9) Region of reversed flow. In the vicinity of $\Psi = 270^{\circ}$, there is an angular region near the hub where the wind velocity exceeds the linear velocity of the in-board blade elements. This results in a relative air flow from the blade trailing edge to the blade leading edge. Some negative lift is therefore created. The boundary of this

reversed flow region can be estimated by setting the equation for the in-plane velocity (Equation 4.1.11) equal to zero. One obtains $x = -\mu \sin \Psi$. The maximum value occurs when $\Psi = 270^{\circ}$, so that then $x = \mu$. But μ never exceeds the value 0.1. Since the minimum value of the blade span variable is $x_1 = 0.15$, the effect of reversed flow on the total lift can then be neglected.

(10) Compressibility effects. The compressibility effects increase both the thrust developed and the power consumed. A maximum air flow velocity of the order of 700 feet per second is encountered at the blade tips. This, however, decreases linearly along the span of the blade to zero feet per second at the centre of the hub. As a first engineering approximation, one can use Prandt-Glauert's relation to account for compressibility effects. Thus the lift curve slope, a, is to be increased by the factor $1/\sqrt{1-M^2}$, where M is a representative mach number for the blade span (say at $x = 2/3$). The factor is thus approximately 1.1. This is considered in taking a = 6/radian.

(11) The downwash angle ϕ is of the order of five degrees. All calculations are therefore based on the substitution $\cos \phi = 1$, and $\sin \phi = \phi$.

(12) Some rotational acceleration of the air takes place when it passes through the rotor discs. This effect is small for one disc and becomes entirely negligible when there are two discs with counter-rotating blades.

(13) The component of the flow velocity along the blade span (radial component) is neglected.

Numerical Computation of Aerodynamic Characterists

All computations of this section have been carried out with the CDC 6400 electronic digital computer at McMaster University. The Fortran IV program used is presented in Appendix 1.

The following aerodynamic parameters are of interest: the thrust; the power consumed; the moments in pitch and roll; and the blade elemental angle of attack as a function of the blade span variable x and the azimuth angle Ψ. All these parameters depend, among other variables, on the distribution of the induced velocity. For the derivation of the various relevant formulas the reader is referred to Ref. 20.

The aerodynamic parameters are computed, and their errors estimated, in terms of the possible error in the induced velocity.

The notation of Section 2 is used. The resultant velocity vector V' at the blade elemental section is resolved into two components. The tangential component U_T lies in the plane of the rotor, while the component U_P is perpendicular to that plane. The components are given by

$$\frac{U_T}{\Omega R} = x + \mu \sin \Psi$$

$$\frac{U_P}{\Omega R} = \lambda + a_o \mu \cos \Psi + \lambda_{o1} Kx \cos \Psi \qquad (4.1.11)$$

Collective Pitch Setting

The thrust and the power are computed for a number of values of the collective pitch setting θ_c in still air. Equations 4.1.12 and 4.1.15 are used. It is found that $\theta_c = 8.5^\circ$ gives a thrust of 96.1 pounds and that this requires 8.66 hp. This is just above the required thrust of 95.0 pounds. The value 8.5° is therefore adopted for the entire analysis.

Thrust

The average value of the thrust is

$$T = \frac{1}{8}\rho a C_o b \Omega^2 R^3 \left((\theta_c t_3 - \lambda t_2 + \mu^2 t_1 \theta_c - B\mu t_2)\right) \qquad (4.1.12)$$

or $T = Y C_T$

This expression is used to compute the thrust for wind speeds up to 60 feet per second and incidences from -20° to $+20^\circ$. The results are shown in Appendix 1, Table 1.

Expect for $\alpha = 20^\circ$, the thrust is seen to increase with increasing wind velocity. At $\alpha = 20^\circ$ the thrust decreases to just below the hovering value of 95 pounds. A change in the collective pitch setting would be needed to keep the thrust above the hovering value. This would somewhat increase the required power.

*In this analysis, μ does not exceed 0.1; θ_{c_r} is zero; and B is very small (which is shown later). Equation 4.1.12 can therefore be simplified to

$$T = YC_T = Y(\theta_{c_R} t_3 - \lambda t_2)$$

This expression can be used for a rapid calculation of the thrust under all wind conditions.

From Equation 4.1.12 it is seen that the thrust depends on the mean induced velocity λ_{o1} as calculated from Glauert's formula. The thrust is thus not affected by the longitudinal variation of the induced velocity. If the mean induced velocity calculated from Glauert's formula is not correct, then there will be an error in the calculated thrust. It is of interest to see, therefore, what percentage error in thrust results from a one percent error in the mean induced velocity. Thus one has from Equation 4.1.12,

$$\frac{\text{Percentage variation in thrust}}{\text{Percentage variation in mean induced velocity}} = -\frac{t_2\lambda_{o1}}{C_T} \qquad (4.1.13)$$

Equation 4.1.13 can be used for all relevant wind conditions. The maximum value (which occurs at zero wind velocity) is -1.5. The percentage error in thrust is therefore up to 1.5 times the percentage error in the mean induced velocity.

Power Required

The power required is given by

$$H.P. = \frac{C_Q \cdot Y \cdot R \cdot}{550} \qquad (4.1.14)$$

where C_Q is the torque coefficient. The power required consists of two parts: the induced power and the profile power. (The induced power is usually about 70 percent of the total power). Thus

$$C_Q = C_T\lambda + \frac{\delta t_4}{a} \qquad (4.1.15)$$

Strictly, δ varies along the blade span because the airfoil (cross-

sectional shape) and the downwash angle ϕ are in general not constant. However, a constant average value can be assumed. This value is 0.007.

Equations 4.1.14 and 4.1.15 are used for the computation of the required power under various wind conditions. The results are shown in Appendix 1, Table 1. It is seen that the variation of the required power with wind velocity and incidence is small. The highest calculated value is 8.79 hp.

Roll Moment

The average roll moment developed by both rotors is

$$\text{Roll moment} = \frac{1}{8}\rho a C_o \frac{b}{2} \Omega^2 R^4 \left(\mu(2\theta_c t_3 - \lambda t_2) + B\left(-t_4 - \frac{3}{4}\mu^2 t_2\right)\right) \quad (4.1.16)$$

or Roll moment = $Y_M \quad C_{MR}$

A positive value indicates a roll to the left. Equation 4.1.16 is used to calculate the roll moment in various wind conditions with no feathering (B=0). Results are shown in Appendix 1, Table 2. The roll moment increases with increasing wind velocity. The wind direction has little effect.

The sign of the roll moment produced by one rotor is opposite to the sign of the roll moment produced by the other (counter-rotating) rotor. The resultant moment may therefore be zero, or it may be a small moment to the left or right.

Pitch Moment

The average pitch moment developed by both rotors is

$$\text{Pitch moment} = \frac{1}{8}\rho a C_{o2} \frac{b}{2} \Omega^2 R^4 \left(K(\lambda_{o1} t_4) + a_o(\mu t_3) + A(t_4 + \frac{1}{4}\mu^2 t_2)\right)$$

$$= Y_M C_{PM} \qquad (4.1.17)$$

A positive value indicates a nose-up moment. Since both rotors develop nose-up moments, the resultant pitch moment is twice the value obtained for a single rotor. The first term in Equation 4.1.17 is the pitch moment produced by the longitudinal variation over the rotor disc of the induced velocity. The second term is the pitch moment produced by the coning angle a_o. The third term is the pitch moment produced by feathering. The third term depends on the feathering angle A. The three terms constitute independent contribution to the total pitch moment. The first two terms are separately computed for the various wind conditions. The results are shown in Appendix 1, Table 2, and in Figure 8. The third term is a control moment; it is discussed in Section 4.2.

It is seen that the contribution to the pitch moment from the coning angle (which is assumed to be one degree) is very small compared with the contribution by the longitudinal variation of the induced velocity. The coning angle is not expected to exceed three degrees. Its contribution to the total pitch moment therefore remains below 7-8 per cent. For this reason, the effect of the coning angle on the pitch moment is from here on neglegted.

For a given value of the wind velocity, the pitch moment is low if the wind incidence is $+20^o$. As the wind incidence decreases, the pitch moment increases and reaches a maximum at a wind incidence

of -20°. The pitch moment is zero in still air. As the wind velocity increases, the parameter K increases asymptotically to the maximum value 1.33. At the same time the induced velocity decreases. At low speeds the increase in K dominates over the decrease in the induced velocity, so that the pitch moment $K\lambda_{o1}t_4$ increases with wind velocity. Having reached its maximum, the pitch moment then decreases with increasing wind velocity. Figure 8 clearly indicates this behaviour. The periscopter operates in the range of wind velocities in which the pitch moment is large and therefore critical.

An examination of Equation 4.1.17 reveals that the calculated value of the pitch moment is sensitive to both the calculated value of K and to the calculated value of the mean induced velocity λ_{o1}.

It follows that for zero or negligible coning angle at every wind condition

$$\frac{\text{Percentage variation of Pitch moment}}{\text{Percentage variation of K}} = 1.0 \qquad (4.1.18)$$

The mean induced velocity affects both the value of K and the pitch moment. One has,

$$\frac{\partial K}{\partial \lambda_{o1}} = \frac{\partial}{\partial \lambda_{o1}} \left(\frac{4/3\ \mu}{(1.2\lambda + \mu)} \right)$$

$$= -1.2\ \frac{4/3\ \mu}{(1.2\lambda + \mu)^2}$$

$$= -0.9\ \frac{K^2}{\mu}$$

and

$$\frac{\text{Percentage variation in Pitch moment}}{\text{Percentage variation in } \lambda_{ol}} = \left(t_4 K + t_4 \lambda \frac{\partial K}{\partial \lambda_{ol}}\right) \frac{\lambda_{ol}}{C_{MP}}$$

$$= \left(1 - 0.9K \frac{\lambda_{ol}}{\mu}\right) \qquad (4.1.19)$$

This ratio has been calculated and is found to be zero near the still air condition. It reaches the value 0.6 at a wind velocity of 60 feet per second.

Blade Stalling

A check has been made on the possibility that stalling occurs on any portion of the blade at some azimuth angle. It is assumed that the stall angle is 12 degrees. It was shown in Section 2.1 that the blade elemental angle of attack is $\theta_c - \phi$, so that for no stall $(\theta_c - \phi) < 12^\circ$ or $\phi > -3.5^\circ$ (Since $\theta_c = 8.5^\circ$). But

$$\phi = \frac{U_P}{U_T} = \frac{\lambda + a_o \mu \cos\Psi + \lambda_{ol} Kx \cos\Psi}{x + \mu \sin\Psi},$$

ϕ is calculated for $\Psi = 0^\circ$, 90°, 180°, and 360°, at the blade points $x = 0.33$, 0.66, and 1.0, for all wind conditions. It is seen that ϕ never goes below -3.5°. One may therefore conclude that no blade stalling occurs. The lowest computed value of ϕ is -1.5°; it occurs at $\phi = 180^\circ$, $x = 1.0$, $V = 60$ feet per second, and $\alpha = -20^\circ$. It is also seen that the most critical region for blade stall, if it should ever occur, is near $\Psi = 180^\circ$. This is on the upstream side of the rotor. The stalling would first begin at the rotor tips.

4.2 The Control Problem

Three modes of control are provided in a periscopter. These are control in pitch, in roll, and in yaw. A rigid feathering rotor should be capable of providing all three controls: pitch and roll control by applying cyclic pitch to the blades, and yaw control by varying the collective pitch setting of one rotor with respect to the other. In this section the question is investigated whether the adopted rigid feathering rotor system can provide the control moments required to neutralize the unbalanced aerodynamic moments, under all relevant wind conditions. In addition, the control power is determined that remains available for manoeuvering, under any wind conditions.

Roll and Pitch Control

The correct feathering angles A and B, for any wind conditions, can be determined by requiring that the net pitch and roll moments developed are both zero. A and B are therefore obtained by setting Equations 4.1.16 and 4.1.17 equal to zero. One obtains

$$A = -\frac{K\lambda_{o1}t_4 + a_o\mu t_3}{t_4 + \frac{1}{4}\mu^2 t_2}$$

$$B = -\frac{(2\theta_c t_3 - \lambda t_2)}{t_4 + \frac{1}{2}\mu^2 t_2}$$

or, since $\frac{1}{4}\mu^2 t_2 \ll t_4$,

$$A = -\frac{K\lambda_{o1}t_4 + a_o\mu t_3}{t_4}$$

$$B = -\frac{(2\theta_c t_3 - \lambda t_2)}{t_4} \qquad (4.2.1)$$

Equations 4.2.1 show that the control angles A and B are respectively proportional to the unbalanced pitch and roll moments. The proportionality constant is the same for A and for B. It was shown in Section 4.1 that the roll moments are almost negligible conpared with the pitch moments. The feathering angle B required for roll control is therefore very small compared with the feathering angle A required for pitch control. Thus, if a feathering mechanism is adequate for pitch control, it is also adequate for roll control. For this reason, it is necessary only to examine the rotor system for pitch control.

The feathering angle A for pitch control has been computed from Equation 4.2.1 for wind velocities up to 60 feet per second. The results are shown in Appendix 1, Table 2, and in Figure 8. Except for a difference in ordinate scale, Figure 8 is the same graph as that obtained for the pitch moment.

The feathering angle A, and therefore the control power, cannot be increased beyond a certain limit. The limit is determined by the beginning of blade stall at the downstream half of the rotor disc. Application of the feathering angle -A results in an increase of the blade elemental angle of attack in the downstream half of the rotor disc and in a decrease of the angle of attack in the upstream half.

Maximum increase occurs at the azimuth position $\Psi = 0^{\circ}$ and is equal to the angle A. Maximum decrease occurs at $\Psi = 180^{\circ}$, and is equal to the angle -A. A continuous increase in the feathering angle -A can give rise to two effects. In the upstream half of the disc, the

blade elemental angle of attack decreases and may become negative, thus causing the local thrust to become negative. This is not harmful because such negative thrust in the upstream half of the disc provides a desired nose-down pitch moment. In the downstream half of the disc the blade elemental angle of attack may exceed the blade section stall angle. Such stall would be accompanied by diminished thrust, increased required power, and by vibrations or flutter. Blade stall should therefore be avoided. This imposes the limitation on the feathering angle A.

If both rotors are provided with individual feathering mechanisms, then each rotor blade must be given feathering angles A as listed in Appendix 1, Table 2. Once the feathering angle A has been selected, the blade elemental angle of attack i can be calculated, for all relevant wind conditions, from the expression

$$i = (\theta_c - A\cos\Psi) - \phi$$

$$= \theta_c - A\cos\Psi - \frac{\lambda + a_o\mu\cos\Psi + \lambda_{o1}K_x\cos\Psi}{x + \mu\sin\Psi} \qquad (4.2.2)$$

Equation 4.2.2 shows that maximum i occurs at $x = 1.0$. One can therefore determine the beginning of stall by computing i at $x = 1.0$. Nevertheless, i is a complicated function of Ψ so that it is difficult to predict the value of Ψ at which stalling begins. Calculations show that i reaches its maximum in the interval $-5^\circ < \Psi < 5^\circ$. One can therefore check for stall without introducing any appreciable error by calculating i at $\Psi = 0^\circ$. Results are shown in Appendix 1, Table 3.

It is seen that i never exceeds 8°, a value much lower than 12°, the stalling angle for the blade section used in the present periscopters. A rotor system with both rotors feathered may therefore be safely used for producing the required control moments in pitch and roll.

Providing each rotor with its own feathering mechanism will present prohibitive mechanical problems. Providing only one rotor with a feathering mechanism, and leaving the other rotor rigid and unfeathered, could be accomplished by a much simpler design. In such a design the feathered rotor must provide sufficient control power to neutralize the unbalanced moment produced by both rotors. This would require feathering angles twice as large as those given in Appendix 1, Table 2. Again, the limitation for these angles is the occurance of blade stall. Calculations have been made, for the blade elemental angle of attack under all relevant wind conditions, for the case when only one rotor is feathered (Appendix 1, Table 3). It is found that no stall occurs for any wind conditions considered. (See Appendix 1, Table 3, and also Figure 8.)

Thus it is possible to neutralise the unbalanced pitch and roll moments developed due to winds by employing only one feathered rotor for control in a periscopter. Mechanical considerations would suggest that the lower rotor should be the one that is feathered.

Yaw Control

Yaw control is easily achieved by varying the collective pitch setting of one rotor. This can be done regardless whether both rotors are feathered or only one rotor is feathered.

Additional Control Power Available for Manoeuvering

An increase of the feathering angle A beyond the value required for neutralizing unbalanced pitch moments will give an additional moment. This moment can be used for manoeuvering the periscopter. The limitation is again that the blade elemental angle of attack must not increase beyond the stall angle at any point on the rotor disc. One thus requires,

$$A_m = (12^\circ - i_{max}) \qquad (4.2.3)$$

where the angle A_m gives the manoeuvering for a configeration in which only one rotor is feathered, for all relevant wind conditions. The values of A_m are tabulated in Appendix 1, Table 3. As one might expect the manoeuvering power has a maximum for hovering in still air. It decreases rapidly as the wind velocity increases.

4.3 Stability Characteristics

The flying qualities of an aircraft largly depend on its inherent stability characteristics. Ideally, an aircraft should be both statically and dynamically stable. Static stability implies that a disturbance of the flight condition is accompanied by forces and moments that tend to return the aircraft to its undisturbed trim state. Static stability does not suffice. The restoring motion may be followed by divergent oscillations. For dynamic stability, these unstable oscillations must be sufficiently damped. Conventional helicopters are dynamically very unstable and are therefore difficult to fly. Their flying qualities are usually improved by the use of a suitably designed automatic control system.

Many sources are available dealing with the stability problem of the helicopter, especially those equipped with articulated (flapping) rotors. (Ref. 10, 13, 17, 18, 20, 22, 23.) Helicopter stability analysis cannot be applied to predict the stability characteristics of the periscopter. The stability and control analysis of the periscopter is effected by the fact that the periscopter is tethered to its ground vehicle. (The cable introduces an additional force, the tension of the cable, and restricts the freedom of motion of the periscopter.)

In this section, an analysis is presented of the periscopter's static and dynamic stability. Certain dynamic instabilities are theoretically predicted, and it is investigated how these instabilities

are affected by the various design and flight parameters of the periscopter. An attempt is made to determine whether the periscopter can be rendered stable with the help of controls. No attempt is made to suggest any specific design for the control system.

The analysis can also be used to predict the effect of various design and flight parameters on the flying qualities of the periscopter. Of particular interest is the effect of the tension of the tether cable. An optimum value for this tension can be estimated. This has an important bearing on the total thrust to be developed by the rotor system. The effect on the stability characteristics of the following additional parameters is discussed: the flight altitude; the distance between the centre of gravity of the flying platform and the point where the cable is attached to it; the height of the rotors above the centre of gravity of the periscopter; the blade tip speed.

The mathematics of dynamic stability is very complex if applied rigorously. Suitable simplying assumptions are therefore made and justified at various stages. Only the motion in the longitudinal plane is considered. This implies that the motion in the lateral plane and the motion in the longitudinal plane can be assumed to be uncoupled. In helicopters, such coupling is believed to be weak and is therefore ignored in simplified analysis. However, Price has shown that this coupling can be important, (Ref. 22). In pericopters, there is ample justification for the assumption that the coupling is weak. The forces and moments produced by the two rotors in the lateral plane are opposite and equal. It can therefore be expected that a longitudinal

motion will not create any appreciable lateral motion. The periscopter has only two degrees of freedom in the longitudnal plane. Two equations of motion must therefore be set up and solved. These equations are formulated and linearized. Linearization implies the assumption that all the perturbations about the trim position are small. Vertical hovering is taken to be the trim position. The resulting linearized ordinary differential equations are analyzed for stability behaviour. The analysis is general, i.e., no particular solution is sought for a particular set of parameters.

ADDITIONAL SYMBOLS USED

A dot on a variable indicates its time derivative.

A variable subscript indicates derivative with respect to that subscript.

A subscript '0' refers to initial trimmed values.

oxyz	set of body axes
u, x, ω	velocities in x, y and z-directions
OXYZ	set of fixed axes
θ, ϕ	lagrangian coordinates for the centre of gravity of periscopter
γ	$(\phi - \theta)$
I	moment of inertia of the periscopter about y-axix
m	mass of the periscopter
W	weight of the periscopter
k_1, k_2, k_3, k_5	constants defined in Appendix 2.2
P	cable tension
D	body drag

M	pitching moment
CM	control moment
B	stability matrix
T_D	time to double the amplutude
T_P	time period of oscillations
V_t	tip speed (Ω R)

Equations of Motion in the Longitudinal Plane

Figure 9 (Appendix 2) shows the model of a periscopter. The model is used for the analysis. The flying platform whose centre of gravity lies at the point o, is attached to the ground by a cable of length ℓ_1. The cable is assumed to be straight and is attached to the platform at a distance ℓ_2 below the centre of gravity. The cable exerts a force P on the periscopter platform by virture of its tension. Both rotor planes are assumed to be at a distance ℓ_3 from the centre of gravity o. Thrust is along the rotor shaft and hence perpendicular to the rotor plane. Since the H - forces of the two rotors amplify each other (rather than cancel) they are included in the analysis. The rotors develop also a pitch moment M about the centre of gravity o. It is assumed that there is a control moment CM about the centre of gravity o. Further, there is body drag D acting on the platform at a distance ℓ_4 below the point o. Figure 9 shows all the forces and moments considered.

Two sets of axes are used. OXYZ is the axis system fixed in space. Point O is at the ground where the cable is attached (see

Figure 9). oxyz is the set of body axes, with ox along the rotor shaft. ϕ and θ are two independent lagrangian coordinates for the centre of gravity o with respect to the fixed coordinate system OXYZ (see Figure 9).

The equations of motion are now written by considering the equilibrium of the centre of gravity. One obtains

$$\begin{aligned} &\text{for x-forces,} && F_{x_i} + T - W \cos\phi - P \cos\gamma = 0 \\ &\text{for z-forces,} && F_{z_i} + W \sin\phi + P \sin\gamma + D + H = 0 \\ &\text{for moments,} && M_i - M + CM + P\ell_2 \sin\gamma + \ell_4 D - H\ell_3 = 0 \end{aligned} \qquad (4.3.1)$$

where F_{x_i} and F_{z_i} are inertia forces in the x and z directions. M_i is the inertia moment. These are evaluated as follows. Considering the motion of the centre of gravity with respect to the fixed coordinate system OXYZ one obtains

$$\begin{aligned} \dot{X} &= \frac{\delta}{\delta t}(\ell_1 \sin\theta + \ell_2 \sin\phi) \\ &= \ell_1\dot{\theta}\cos\theta + \ell_2\dot{\phi}\cos\phi \qquad (4.3.2) \\ \dot{Z} &= -(\ell_1\dot{\theta}\sin\theta + \ell_2\dot{\phi}\sin\phi) \\ Q &= -\dot{\phi} \end{aligned}$$

The motion of the centre of gravity with respect to the body axes oxyz is given by

$$\begin{aligned} u &= \dot{x} = \dot{X}\sin\phi + \dot{Z}\cos\phi \\ \omega &= \dot{z} = \dot{X}\cos\phi - \dot{Z}\sin\phi \\ q &= -\dot{\phi} \end{aligned}$$

Or, using Equation 4.3.2,

$$u = \ell_1 \dot{\theta} \text{ Sin } \gamma$$

$$\omega = \ell_1 \dot{\theta} \text{ Cos } \gamma + \ell_2 \dot{\phi} \qquad (4.3.3)$$

$$q = -\dot{\phi}$$

The inertia forces are given by

$$F_{x_i} = -m (\dot{u} + \omega q)$$

$$F_{z_i} = -m (\dot{\omega} - uq)$$

$$M_i = - I\dot{q}$$

or, using Equation 4.3.3,

$$F_{x_i} = -m (\ell_1 \ddot{\theta} \text{ Sin } \gamma - \ell_1 \dot{\theta}^2 \text{ Cos } \gamma - \ell_2 \dot{\phi}^2)$$

$$F_{z_i} = -m (\ell_1 \ddot{\theta} \text{ Cos } \gamma + \ell_1 \dot{\theta}^2 \text{ Sin } \gamma + \ell_2 \ddot{\phi}) \qquad (4.3.4)$$

$$M_i = I\ddot{\phi}$$

Using Equation 4.3.4, the equations of motion (Equation 4.3.1) reduce to

$$-m(\ell_1 \ddot{\theta} \text{ Sin } \gamma - \ell_1 \dot{\theta}^2 \text{ Cos } \gamma - \ell_2 \dot{\phi}^2) + T - W \text{ Cos } \phi - P \text{ Cos } \gamma = 0$$

$$-m(\ell_1 \ddot{\theta} \text{ Cos } \gamma + \ell_2 \ddot{\phi} + \ell_1 \dot{\theta}^2 \text{ Sin } \gamma) + W \text{ Sin } \phi + P \text{ Sin } \gamma + D + H = 0$$

$$I\ddot{\phi} + (-M + P\ell_2 \text{ Sin } \gamma + \ell_4 D - H\ell_3) + CM = 0$$

The first equation is used to eliminate P from the other two. One

obtains

$$-m((\ell_1 \text{Cos } \gamma + \ell_1 \text{ Tan } \gamma \text{ Sin } \gamma)\ddot{\theta} + \ell_2\ddot{\phi} - \ell_2\dot{\phi}^2 \text{ Tan } \gamma) + T \text{ Tan } \gamma$$

$$+ W(\text{Sin } \phi - \text{Cos } \phi \text{ Tan } \gamma) + D - H = 0 \qquad (4.3.5)$$

$$I\ddot{\phi} + (-M + \ell_4 D - H\ell_3 + CM) - m\ell_2 (\ell_1\ddot{\theta} \text{ Sin } \gamma - \ell_1\dot{\theta}^2 \text{ Cos } \gamma - \ell_2\dot{\phi}^2)$$

$$+ T\ell_2 \text{ Tan } \gamma - W\ell_2 \text{ Cos } \phi \text{ Tan } \gamma = 0$$

The two equations (Equation 4.3.5) together determine the motion of the periscopter at any trim position given by θ and ϕ. The equations are extremely non-linear and are not used as such in the analysis.

Equations of Perturbed Motion

Equations 4.3.5 are linearised by assuming small perturbations $\Delta\theta$ and $\Delta\phi$, about the trim values θ and ϕ. Thus

$$\theta = \theta + \Delta\theta$$

$$\phi = \phi + \Delta\phi$$

Since the perturbations are small all second and higher order quantities can be neglected. Thus the aerodynamic quantities appearing in Equation 4.3.5 are expanded a Taylor series and only the first order terms are retained. For example,

$$T = To + \frac{\delta T}{\delta \theta}\Delta\theta + \frac{\delta T}{\delta \phi}\Delta\phi + \frac{\delta T}{\phi \theta}\dot{\Delta\theta} + \frac{\delta \dot{T}}{\delta \phi}\dot{\Delta\phi}$$

The trigonometric functions in Equation 4.3.5 are expanded as follows

$$\text{Cos } (\phi + d\phi) = \text{Cos } \phi - \text{Sin } \phi \, \Delta\phi$$

$$\text{Sin } (\phi + d\phi) = \text{Sin } \phi + \text{Cos } \phi \, \Delta\phi$$

$$\text{Tan}\ (\phi + d\phi) = \text{Tan}\ \phi + \text{Sec}^2\ \Delta\phi$$

$$(\dot{\phi} + \Delta\dot{\phi})^2 = \dot{\phi}^2 + 2\dot{\phi}\,\Delta\dot{\phi}$$

$$(\dot{\phi} + \Delta\dot{\phi})\ \text{Tan}\ (\phi + \Delta\phi) = \dot{\phi}^2\ \text{Tan}\ \phi + \dot{\phi}^2\ \text{Sec}^2\phi + 2\dot{\phi}\ \text{Tan}\ \phi\ d\dot{\phi}$$

$$\text{Tan}\ (\gamma + d\gamma)\ \text{Sin}\ (\gamma + d\gamma) = \text{Tan}\ \gamma\ \text{Sin}\ \gamma + (\text{Tan}\ \gamma\ \text{Sec}\ \gamma + \text{Sin}\ \gamma)\ \Delta\gamma$$

$$(\ddot{\theta} + \Delta\ddot{\theta})\ \text{Sin}\ (\gamma + d\gamma) = \ddot{\theta}\ \text{Sin}\ \gamma + \ddot{\theta}\ \text{Cos}\ \gamma\ \Delta\gamma + \text{Sin}\ \gamma\ \Delta\ddot{\theta}$$

Using these relations, the equations of motion (Equation 4.3.5) reduce to

$$\begin{aligned}
&-m\ell_1(\text{Cos}\ \gamma + \text{Tan}\ \gamma\ \text{Sin}\ \gamma)\ \Delta\ddot{\theta} + (T\ \text{Tan}\ \gamma + D + H)_{\dot{\theta}}\ \Delta\dot{\theta} \\
&+ (-M\ell_1\ddot{\theta}\ \text{Sin}\ \gamma + m\ell_1\ddot{\theta}\ \text{Tan}\ \gamma\ \text{Sec}\ \gamma + \ell_1\ddot{\theta}\ \text{Sin}\ \gamma - m\ell_2\dot{\phi}^2\ \text{Sec}^2\gamma \\
&+ T_\theta\ \text{Tan}\ \gamma - T_o\ \text{Sec}^2\gamma + W\ \text{Sec}^2\gamma\ \text{Cos}\phi + D_\theta + H_\theta)\ \Delta\theta \\
&+ (\ell_2)\ \Delta\ddot{\phi} + (2m\dot{\phi}\ell_2\ \text{Tan}\ \gamma + T_{\dot{\phi}}\ \text{Tan}\ \gamma + D_{\dot{\phi}} + H_{\dot{\phi}})\ \Delta\dot{\phi} \\
&+(m\ell_1\ddot{\theta}\ \text{Sin}\ \gamma - m\ell_1\ddot{\theta}\ \text{Tan}\ \gamma\ \text{Sec}\ \gamma - m\ell_1\ddot{\theta}\ \text{Sin}\ \gamma + m\ell_2\ \text{Sec}^2\gamma\ \dot{\phi}^2 \\
&+ T_\phi\ \text{Tan}\ \gamma + T_o\ \text{Sec}^2\gamma + W\ \text{Cos}\ \phi - W\ \text{Sec}^2\gamma\ \text{Cos}\ \phi \\
&+ W\ \text{Tan}\ \gamma\ \text{Sin}\ \phi + D_\phi + H_\phi)\ \Delta\phi = 0
\end{aligned}$$

and (4.3.6)

$$\begin{aligned}
&I\ \Delta\ddot{\phi} + ((-M + \ell_4 D - \ell_3 H + CM)_{\dot{\phi}} + 2m\ell_2^2\dot{\phi} + \ell_2 T_{\dot{\phi}}\ \text{Tan}\ \gamma)\ \Delta\dot{\phi} \\
&+ ((-M + \ell_4 D - \ell_3 H + CM)_\phi - m\ell_1\ell_2\ddot{\theta}\ \text{Cos}\ \gamma - m\ell_1\ell_2\ \dot{\theta}^2\ \text{Sin}\ \gamma + \ell_2 T_\phi\ \text{Tan}\ \gamma \\
&+ \ell_2 T_o\ \text{Sec}^2\gamma + W\ell_2\ \text{Sin}\ \phi\ \text{tan}\ \gamma - W\ell_2\ \text{Cos}\ \phi\ \text{Sec}^2\gamma)\ \Delta\phi \\
&+ (-m\ell_1\ell_2\ \text{Sin}\ \gamma)\ \Delta\ddot{\theta} + ((-M + \ell_4 D - \ell_3 H + CM)_{\dot{\theta}} + 2m\ell_1\ell_2\dot{\theta}\ \text{Cos}\ \gamma \\
&+ \ell_2 T_{\dot{\theta}}\ \text{Tan}\ \gamma)\ \Delta\dot{\theta} + ((-M + \ell_4 D - \ell_3 H + CM)_\theta + m\ell_1\ell_2\ddot{\theta}\ \text{Cos}\ \gamma \\
&- m\ell_1\ell_2\dot{\theta}^2\ \text{Sin}\ \gamma + \ell_2 T_\theta\ \text{Tan}\ \gamma - \ell_2 T_o\ \text{Sec}^2\gamma \\
&+ W\ell_2\ \text{Cos}\ \phi\ \text{Sec}^2\gamma)\ \Delta\phi = 0.
\end{aligned}$$

Since one is interested in analyzing the case where the periscopter is hovering in vertical altitude, the trim conditions can be written as,

$$\theta = \dot{\theta} = \ddot{\theta} = 0,$$
$$\phi = \dot{\phi} = \ddot{\phi} = 0,$$

so that $\gamma = 0$.

For these trim conditions, the equations of perturbed motion as given by equation 4.3.6 simplify to

$$(m\ell_2)\,\Delta\ddot{\phi} + (-D - H)_{\dot{\phi}}\,\Delta\dot{\phi} + (-W - P_o - D_\phi - H_\phi)\,\Delta\phi$$
$$+ (m\ell_1)\,\Delta\ddot{\theta} + (-D - H)_{\dot{\theta}}\,\Delta\dot{\theta} + (P_o - D_\theta - H_\theta)\,\Delta\theta = 0$$

and

$$I\,\Delta\ddot{\phi} + (-M + CM + \ell_4 D - \ell_3 H)_{\dot{\phi}}\,\Delta\dot{\phi} + ((-M + CM - \ell_3 H + \ell_4 D)_\phi + \ell_2 P_o)\,\Delta\phi$$
$$+ (0)\,\Delta\ddot{\theta} + (-M + CM + \ell_4 D - \ell_3 H)_{\dot{\theta}}\,\Delta\dot{\theta} + ((-M + CM - \ell_3 H + \ell_4 D)_\theta - \ell_2 P_o)\,\Delta\theta = 0$$

or, on introducing of symbols for the coefficients,

$$a_1\,\Delta\ddot{\phi} + b_1\,\Delta\dot{\phi} + c_1\,\Delta\phi + a_2\,\Delta\ddot{\theta} + b_2\,\Delta\dot{\theta} + c_2\,\Delta\theta = 0$$

and (4.3.7)

$$a_2\,\Delta\ddot{\phi} + b_3\,\Delta\dot{\phi} + c_3\,\Delta\phi + a_4\,\Delta\ddot{\theta} + b_4\,\Delta\dot{\theta} + c_4\,\Delta\theta = 0$$

The coefficients a_1, b_1, c_1, a_2, b_2, c_2, a_3, b_3, c_3, a_4, b_4, c_4 are functions of various stability derivatives. These are derived in Appendices 2.1 and 2.2. The coefficients of Equation 4.3.7 are evaluated in Appendix 2.3.

Equations 4.3.7 are written in matrix form as

$$\begin{bmatrix} \Delta\phi \\ \Delta\theta \\ \Delta\dot{\phi} \\ \Delta\dot{\theta} \end{bmatrix} = B \begin{bmatrix} \Delta\dot{\phi} \\ \Delta\dot{\theta} \\ \Delta\ddot{\phi} \\ \Delta\ddot{\theta} \end{bmatrix}$$

where B is the 4 X 4 matrix

$$B = \begin{bmatrix} 0 & 0 & 1 & 0 \\ 0 & 0 & 0 & 1 \\ -\frac{c_3}{a_3} & -\frac{c_4}{a_3} & -\frac{b_3}{a_3} & -\frac{b_4}{a_3} \\ \left(\frac{a_1c_3}{a_2a_3} - \frac{c_1}{a_2}\right) & \left(\frac{a_1c_4}{a_2a_3} - \frac{c_2}{a_2}\right) & \left(\frac{a_1b_3}{a_2a_3} - \frac{b_1}{a_2}\right) & \left(\frac{a_1b_4}{a_2a_3} - \frac{b_2}{a_2}\right) \end{bmatrix} \quad (4.3.9)$$

The characteristic equation of B is

$$a\lambda^4 + b\lambda^3 + c\lambda^2 + d\lambda + e = 0 \quad (4.3.10)$$

where

$$a = 1.0$$

$$b = \left(\frac{b_3}{a_3} - \frac{a_1b_4}{a_2a_3} + \frac{b_2}{a_2}\right) \text{Sec}^{-1}$$

$$c = \left(\frac{1}{a_2a_3}(b_2b_3 - b_1b_4) + \frac{c_3}{a_3} + \frac{c_2}{a_2} - \frac{a_1c_4}{a_2a_3}\right) \text{Sec}^{-2} \quad (4.3.10a)$$

$$d = \frac{1}{a_2a_3}\left((b_2c_3 + b_3c_2) - (b_4c_1 + b_1c_4)\right) \text{Sec}^{-3}$$

$$e = \left(\frac{1}{a_2a_3}(c_2c_3 - c_1c_4)\right) \text{Sec}^{-4}.$$

The problem of finding the stability characteristics of the periscopter is now reduced to finding the nature of the roots of the polynomial Equation 4.3.10, which is usually referred to as the stability

polynomial. The system is stable if the real parts of all roots of the stability polynomial are negative. Necessary and sufficient conditions for the real part of the roots to be negative are: (a) the coefficients a, b, c, d, e must be positive; and (b) Routh's determinants R_1 and R_2 must be positive where,

$$R_1 = (bc - ad)$$

$$R_2 = d(bc - ad) - b^2e.$$

However, the static stability actually depends only on the sign of the coefficient e, for static stability e must be positive.

The analysis so far developed is sufficient for finding the stability characteristics of any periscopter design operating under any wind conditions. Given the design parameters and operating and conditions, Appendix 2 can be used to evaluate the coefficients in the equations of motion, Equation 4.3.7. Once the coefficients are known, it is easy to evaluate the coefficients of the stability polynomial, Equation 4.3.10, and from this Routh's determinants R_1 and R_2. The calculation determines whether the periscopter is stable. If a digital computer is used, one can find the actual roots of the polynomial, Equation 4.3.10, as given by the eigenvalues of the matrix B. One can then evaluate the damping (given by the time to double or half the amplitude of unstable or stable oscillations, respectively) and the frequency of the oscillations. In addition, it is easy to vary any selected parameter, say the cable tension P_o, and study the effect on the stability behaviour. However, the interaction of various

parameters is sufficiently complex to render such broad generalizations rather dangerous.

In order to gain some physical insight into the problems and attempt to obtain some broad generalizations for the stability behaviour, one has to deal with the problem analytically. This is not a very inviting proposition in view of the extensive complexities involved. A certain amount of simplification results for zero wind conditions. In the following pages, the problem is analyzed for zero wind conditions.

Stability in Zero-Wind Conditions

For the periscopter hovering in still air (i.e. V = 0), the coefficients of the stability polynomial, Equation 4.3.10, simplify to (see Appendix 2.4)

$$a = 1.0$$

$$b = \frac{1}{I\Omega R}\left(\frac{I}{m}k_1 + \ell_3(k_2 + \ell_3 k_1)\right) + \left(\frac{k_5 - \ell_3 k_3}{I}A_\phi^\bullet\right)$$

$$- \left(\frac{\ell_2}{I\ell_1}(k_5 - \ell_3 k_3) + \frac{k_3}{m\ell_1}\right)A_\theta^\bullet)\ Sec^{-1}$$

$$c = P_o\left(\frac{\ell_2}{I} + \frac{1}{m\ell_1} + \frac{\ell_2^2}{\ell_1 I}\right) + \frac{1}{Im\Omega R}(k_1(k_5 - \ell_3 k_3) + k_3(k_2 + \ell_3 k_1)$$

$$\left(A_\phi^\bullet - \frac{\ell_2 + \ell_3}{\ell_1}A_\theta^\bullet\right) + \frac{k_5 - \ell_3 k_3}{I}A_\phi)$$

$$- \left(\frac{k_3}{m\ell_1} + \frac{\ell_2}{\ell_1 I}(k_5 - \ell_3 k_3)\right)A_\theta\ Sec^{-2}$$

$$d = \frac{P_o}{mI\Omega R}\left(\ell_2 k_1 + \frac{(k_2 + \ell_3 k_1)(\ell_2 + \ell_3)}{\ell_1} + (k_2 + \ell_3 k_1)\right)$$

$$+ \frac{\ell_3(\ell_2 + \ell_3)}{\ell_1} k_1 + \frac{W}{P_o}(k_2 + \ell_3 k_1))$$

$$+ \frac{P_o}{mI\ell_1} (((k_5 - \ell_3 k_3) - \ell_2 k_3) (A_\theta^\cdot + A_\phi^\cdot) + \frac{W}{P_o}(k_5 - \ell_3 k_3) A_\theta^\cdot))$$

$$+ \frac{1}{Im\Omega R} (k_1(k_5 - \ell_3 k_3) + k_3(k_2 + \ell_3 k_1)) (A_\phi - \frac{\ell_2 + \ell_3}{\ell_1} A_\theta) \text{ Sec}^{-3}$$

$$e = - \frac{W P_o \ell_2}{Im\ell_1} + \frac{P_o}{Im\ell_1} ((k_5 - \ell_3 k_3 - \ell_2 k_3) (A_\theta + A_\phi)$$

$$+ (\frac{W}{P_o} (k_3 - \ell_3 k_3)) A_\theta) \text{ Sec}^{-1} \qquad (4.3.11a)$$

Much simplification results by assuming $k_3 = 0$. This implies that the coning angle is zero. The assumption does not modify the stability characteristics of the periscopter when flying without controls, since k_3 appears only in the control terms of Equation 4.3.11a. Equation 4.3.11a reduce to

$$a = 1.0$$

$$b = \frac{1}{I\Omega R} (\frac{I}{m} k_1 + \ell_3(k_2 + \ell_3 k_1)) + \frac{k_5}{I} (A_\phi^\cdot - \frac{\ell_2}{\ell_1} A_\theta^\cdot)$$

$$c = P_o(\frac{\ell_2}{I} + \frac{\ell_2^2}{I\ell_1} + \frac{1}{m\ell_1}) + \frac{1}{Im\Omega R} (k_1 k_5 (A_\phi^\cdot - \frac{\ell_2 + \ell_3}{\ell_1} A_\theta^\cdot)$$

$$+ \frac{k_5}{I} (A_\phi - \frac{\ell_2}{\ell_1} A_\theta))$$

$$d = \frac{P_o}{Im\Omega R} ((k_2 + \ell_3 k_1) (1 + \frac{W}{P_o}) + (\frac{\ell_2 + \ell_3}{\ell_1} (k_2 + \ell_3 k_1 + \ell_2 k_1)$$

$$+ \ell_2 k_1))$$

$$+ \left(\frac{P_o}{Im\ell_1} k_5 \left((1 + \frac{W}{P_o}) A_\theta^{\cdot} + A_\phi^{\cdot} \right) + \frac{k_1 k_5}{Im\Omega R} \left(A_\phi - \frac{\ell_2 + \ell_3}{\ell_1} A_\theta\right)\right)$$

$$e = \frac{P_o}{Im\ell_1} (- W\ell_2) + \frac{P_o}{Im\ell_1} \left(k_5 \left((1 + \frac{W}{P_o}) A_\theta + A_\phi \right)\right)$$

and

$$R_1 = bc - ad$$

$$R_2 = d(bc - ad) - be^2 , \qquad (4.3.11)$$

Static stability: In order that the periscopter be statically stable in the absence of controls, one must have

$$e > 0$$

or

$$- \frac{\ell_2 P_o W}{Im\ell_1} > 0$$

or

$$\ell_2 < 0 \qquad (4.3.12)$$

Thus if the cable is attached at a point above the centre of gravity of the periscopter, the machine is statically stable. It may still be dynamically unstable. On the other hand, if the cable is attached at a point below the centre of gravity, the periscopter is both statically and dynamically unstable. Static stability can always be obtained by making a proper choice of the positional controls A_ϕ and A_θ.

Dynamic stability: In order that the system be dynamically stable, the coefficients a, b, c, d, e, and also R_1 and R_2, must be

positive. One first investigates the system for the case where no controls are used. For c and e to be simultaneously positive, it can be shown that the inequality must hold

$$-\frac{I}{m\ell_1^2} < \ell_2 < 0 .$$

Since ℓ_1 is of the order of 100 to 600 feet, ℓ_2 must for all practical purposes be zero. For $R_1 > 0$,

$$bc - ad > 0$$

or

$$\frac{P_o}{I\Omega Rm\ell_1}\left(\frac{I}{m}k_1 + \ell_3(k_2 + \ell_3 k_1)\right) - \frac{P_o}{Im\Omega R}\left((k_2 + \ell_3 k_1)(1 + \frac{W}{P_o})\right.$$

$$\left. + \frac{\ell_3}{\ell_1}(k_2 + \ell_3 k_1)\right) > 0$$

or

$$\ell_1 < \frac{I\,k_1}{m(1 + \frac{W}{P_o})(k_2 + \ell_3 k_1)} \backsim 0.01 \text{ feet.} \qquad (4.3.13)$$

Since inequality 4.3.13 is never satisfied in practice, R_1 is always negative, and hence the periscopter is always dynamically unstable.

It seems possible, nevertheless, to make the system stable by a suitable choice of controls, i.e., by a suitable choice of $A_\theta^\bullet$, $A_\phi^\bullet$, A_θ and A_ϕ. In fact, many combinations of $A_\theta^\bullet$, $A_\phi^\bullet$, A_θ and A_ϕ can render the system stable. One such combination is of interest. One has

$$-k_5 A_\phi^\bullet = \frac{\ell_2 + \ell_3}{\Omega R}(k_2 + \ell_3 k_1)$$

$$- k_5 A_\theta^{\cdot} = \frac{\ell_1}{\Omega R} (k_2 + \ell_3 k_1) \qquad (4.3.14)$$

and

$$- k_5 A_\phi = P_o \ell_2$$

$$- k_5 A_\theta = -P_o \ell_2 \ .$$

These controls can be achieved with the help of suitable rate and displacement gyros. Need for positional control is minimised by letting either ℓ_2 or P_o approach zero. Such gyros can be suitably coupled to the swash plate. Thus, it seems possible to achieve hands-off stability with a swash plate - gyro combination. With these controls (Equation 4.3.14), the coefficients become

$$\begin{aligned} a &= 1.0 \\ b &= \frac{k_1}{m\Omega R} \quad 0.01 \text{ Sec}^{-1} \\ c &= \frac{P_o}{m\ell_1} \quad 0.01 \text{ Sec}^{-2} \\ d &= 0 \\ e &= 0 \\ R_1 &= \frac{k_1 P_o}{m^2 \ell_1 \Omega R} \\ R_2 &= 0 \ . \end{aligned} \qquad (4.3.15)$$

Hence, the system is always stable. Equations 4.3.15 represent only one mode of long period (the time period is $\frac{2\pi}{c}$) oscillations which is very poorly damped (the time to half the amplitude is $\frac{\text{Ln } 2}{b}$). It can be shown that Equations 4.3.14 are compatible with the physics of

the problem. Let dA be the value of the control angle used, dV be the horizontal velocity of the rotor tip path plane. Then

$$-k_5\, dA = -\text{ control moment} = -k_5(dA_\phi^{\cdot}\, d\dot{\phi} + dA_\theta^{\cdot}\, d\dot{\theta})$$

$$= \left(\frac{(\ell_2 + \ell_3)d\dot{\phi}}{R} + \frac{\ell_1\, d\dot{\theta}}{R}\right)(k_2 + \ell_3 k_1)$$

$$= \frac{dV}{R}(k_2 + \ell_3 k_1)$$

= unbalanced moments produced due to finite $\dot{\theta}$ and $\dot{\phi}$

(4.3.14b)

Similarly

$$-k_5\, dA = -\text{ control moment}$$

$$= -k_5(dA_\phi\, d\phi + dA_\theta\, d\theta)$$

$$= P\ell_2\, d\phi - P\ell_2\, d\theta$$

$$= P\ell_2(d\phi - d\theta)$$

$$= P\ell_2\, d\gamma$$

= unbalanced moments produced due to finite γ.

Effect of P_o, ℓ_1 and ℓ_2: An analysis is made to evaluate the effect of P_o, ℓ_1 and ℓ_2, on the stability characteristics of the

periscopter when flying without any controls.

According to Equations 4.3.11, ℓ_1 and ℓ_2 influence only the coefficients c and e (the effect on d is smaller by at least two orders of magnitude). P_o also influences c and e. It also influences, in addition, the coefficient d. The influence is of the order $\frac{P_o}{W}$ and should therefore not be ignored.

One should be able to study the effect of ℓ_1, ℓ_2 and P_o, on the stability behaviour by studying the behaviour of the roots of the stability equation (Equation 4.3.10) when c and e are varied while a, b and d, are kept constant. For normal ranges of the various variables, one can take a = 1.0, b = 0.75 and d = 20.0. (A check made shows that the general nature of the stability behaviour does not change with a small variation in the assumed values of b and d.) With these values of a, b and d, the coefficients c and e are both varied from -3 to +3. This includes a wide range of P_o, ℓ_1 and ℓ_2. Roots of the stability equation, Equation 4.3.10, have been computed using the digital computer. Two roots are real, representing a uniform convergence or divergence of motion. The other two roots form a complex pair, representing an oscillatory motion. There are thus three distinct modes of motion. As a measure of the rate of divergence or convergence of each mode, the time to double or half the amplitude is calculated ($T_D = \frac{\text{Ln } 2}{\text{real part}}$). The time period of the oscillatory mode has also been computed ($T_P = 2\pi/$ imaginary part). The results are presented in the form of graphs (Appendix 2, Figures 10, 11, 12).

The first mode is a uniform rapid convergence. Time to half the amplitude varies between 0.2 and 0.28 seconds, so that this mode dies our rapidly.

The second mode is shown in Appendix 2, Figure 10. It uniformly converges or diverges depending on whether ℓ_2 is negative or positive. The time to double the amplitude is greater than 15 seconds for normal operating values of P_o and ℓ_1($e \lesssim -0.5$). However, for a combination of high P_o($\lesssim$ 25 pounds), low flight altitude ($\approx$ 50 feet), and moderately positive ℓ_2($\lesssim$ 1 foot), the oscillation diverges very rapidly ($T_D \lesssim$ 1 second). This could be one reason why the periscopter test models have been so difficult to fly. (They were flown at a height of 50 feet). The rapid divergence can be avoided by letting either ℓ_2 or P_o approach zero.

Figures 11 and 12 give T_D and T_P for the unstable oscillatory mode. The time period is fairly large ($\approx$ 3 seconds), but the divergence is very rapid ($T_D \lesssim$ 0.6 seconds). The general character of the unstable oscillations does not change with the variation in P_o, ℓ_2 or ℓ_1.

The magnitude of P_o has a direct influence on the effect that ℓ_1 and ℓ_2 have on the character of the oscillations. For very low P_o(0 to 5 pounds), the magnitudes of c and e are only marginally affected by ℓ_1 and ℓ_2, and hence ℓ_1 and ℓ_2 do not appreciably alter the character of the oscillations. This should, of course, be expected even from a physical point of view. Increase in P_o has the

effect of amplifying the effect of ℓ_2 and ℓ_1.

ℓ_1 has no appreciable effect on the oscillatory mode. On the other hand, ℓ_2 seems to strongly effect both the frequency and the rate of divergence, except at very low magnitudes of P_o. At moderate values of P_o ($\approx$ 20 pounds), a variation of ±1 foot in ℓ_2 results in a variation of ±4 in the coefficient c. This means that as the cable junction is moved up, the frequency decreases and the rate of divergence increases (see Figures 11 and 12). This suggests a large positive value for ℓ_2.

Evaluation of the influence of P_o, when ℓ_1 and ℓ_2 are kept constant, must also include the variation of d. Ignoring as a first approximation any large variation of d, an increase in P_o results in an increase in frequency and in T_D for positive ℓ_2, and a decrease in frequency and in T_D for negative ℓ_2 (see Figures 11 and 12).

Effect of tip speed ($V_t = \Omega R$), solidity ratio ($\sigma = \frac{b\,C_o}{\pi R}$), and ℓ_2: According to the Equations 4.3.11, these three parameters influence only the coefficients b and d. One should thus be able to study the effect of these parameters on the stability characteristics by keeping a, c and e, constant and letting b and d vary.

Two sets of values are adopted for a, c and e: a = 1.0, c = +2.0, e = -1.0 (for positive ℓ_2); and a = 1.0, c = -2.0 e = 1.0 (for negative ℓ_2). The coefficient b is varied from 0.5 to 1.1. The coefficient d is varied from 12.0 to 24.0. This includes a sufficiently wide range of working parameters. Equation 4.3.10

has been solved numerically. The resulting four roots represent three modes of motion. T_D and T_P have been computed. The results are shown in Figures 13 and 14 for the oscillatory mode.

The first mode is a uniform rapid convergence with a half time of about 0.25 seconds. The second mode is a uniform convergence or divergence depending upon whether ℓ_2 is negative or positive, respectively. For the values of coefficients considered, the time to double the amplitude in divergence does not exceed 8 seconds.

The third mode is an unstable oscillatory mode. T_D and T_P are shown in Figures 13 and 14. T_P is of the order of 3 seconds. T_D is of the order of 0.75 seconds. Variation in tip speed, solidity, or ℓ_3, does vary the values of T_P and T_D, but the variation is not large enough to change the general character of the oscillations.

The value of b is strongly affected by the value of ℓ_3. On the other hand, d is a weak function of ℓ_3. An increase in the value of ℓ_3 thus results in an increase in T_D, while the frequency of oscillation remains unchanged. Thus increasing ℓ_3 has a desirable influence on the stability characteristics.

The tip speed V_t and the solidity influence the values of the coefficients b and d in an identical manner. According to Figure 14, an increase in these parameters is associated with an increased frequency of oscillation. On the other hand, increasing b increases T_D, while increasing d decreases T_D. It nevertheless appears from Figure 13 that the effect of increasing d is more pronounced. One

should therefore expect that T_D increases with increasing V_t and σ.

5. DISCUSSION

The foregoing analysis has demonstrated the feasibility of adopting a rigid feathering rotor system for the periscopter. The rigid feathering system in a periscopter results in improved aerodynamics, controls, and handling. Also, general principles for the analysis of periscopter rotors have been developed.

For a periscopter, the most critical operational parameter is the unbalanced aerodynamic pitch moment generated in the rotor system. Parameters such as thrust, power, rolling moments, etc., have little importance. According to Section 4.1, the pitch moment is almost entirely a consequence of the variation of induced velocity in the longitudinal plane. Thus, the estimation of this asymmetry of the induced velocity in the longitudinal plane should be the major concern of any aerodynamic analysis performed for the periscopter rotors. In the present analysis, a linear distribution as suggested by Glauert, has been used (Equation 2.2.3). The distribution may not actually be linear, especially at the lower rotor. This longitudinal variation of the induced velocity is a function of the wind velocity and incidence and of the load distribution over the rotor disc (and hence the blade geometry). Theortical evaluation of these factors is difficult. There is therefore a need for experimental determination of the induced velocity in the longitudinal plane for the configeration of two coaxial counter-rotating rotors.

If the distribution of the induced velocity is assumed to be linear, it can be represented by the parameter K(see Equation 2.2.4). Equation 4.1.18 shows that the pitch moment is sensitive to the value of K. One must therefore excercise caution when choosing a particular formula for K. Evaluation of the induced velocity in the longitudinal plane has not received much attention in the literature. This is understandable because for an aerodynamic analysis of helicopter rotors the longitudinal asymmetry of the induced velocity is of little concern.

The pitch moment is a weak function of the mean induced velocity (see Equation 4.1.19). Equation 4.1.9 should therefore suffice for the calculation of the mean induced velocity. The same mean induced velocity should also suffice for the calculation of thrust, power, etc. The wind direction has an appreciable influence on the magnitude of the pitch moment produced, especially for wind velocities greater than 30 feet per second (see Figure 8). It would therefore be erroneous to base the analysis only on the horizontal wind conditions.

Since the interference effects associated with the separation of the two rotors are not well understood, it is desirable to keep the separation as small as possible. This is especially important if no experimental determination of the pitch moment is planned. The assumption that the two discs lie in the same plane leads to a conservative estimate of the thrust. This is because the induced velocity has a maximum when the two discs coincide.

The analysis has also shown that such factors as coning angle,

rolling moment, lateral variation of the induced velocity, area of reversed flow, etc., have no appreciable aerodynamic significance. These quantities can thus be ignored in the analysis for periscopter rotors.

Controls: A very simple control system consisting of a swash plate mechanism for the lower rotor only, is adequate for balancing the unbalanced moments in pitch and roll. The bail mechanism of the present periscopter models, therefore can be dispensed with. This may result in a reduction of the periscopter's weight. Yaw control is also attained by the swash plate, and ground equipment currently used for yaw control can be dispensed with. In such a design, one would not be able to use collective pitch control for thrust control. Thus it is desirable to incorporate some means of varying the power consumed by the upper rotor, so that the collective pitch could then be successfully utilised for ascending, decending, and also for the control of the tension in the cable. This would be very useful because the cable tension is expected to influence the flying qualities.

The control power of the rotor is limited by the onset of stall at the blade tips at $\Psi = 0^{\circ}$. One should thus be able to increase the control power in the following ways: (a) by twisting the blades, so that the geometric angle of incidence is reduced towards the blade tips. This has also the desirable influence of making the load distribution over the blade more uniform; (b) by using an airfoil with better stalling characteristics; (c) the control moment is given by $Y_M A t_4$, for the tapered blades considered $t_4 = 0.58$, for untapered blades

$t_4 = 0.84$. Thus untapered blades would give higher control moment per degree of feathering angle A. (Untapered blades would require a lower C_o, thus Y_M is decreased. But the increase in t_4 dominates). However, tapering of the blades has no influence on the feathering angle required to balance the unbalanced moments. For a rigid feathering rotor, it is desirable to have blades that are twisted but untapered. On the other hand, if the bail mechanism is used for control, one wants to have minimum pitch moment developed. Thus the blades are required to be tapered. It is of interest to note that the blade geometry is to be determined by the considerations of controls, rather than by the considerations of aerodynamic efficiency.

In the control system suggested, the stall does not occur at any wind condition. In fact, the incidence angle i never exceeds ten degrees. Thus any error in the computed value of pitch moment (due to the lack of theoretical knowledge of longitudinal distribution of induced velocity) may not affect the periscopter's performance.

Using feathering of blades, rather than a bail mechanism, gives a complete freedom in the choice of the cable tension and of ℓ_2. These two factors have important influence on the flying qualities, and hence should not be constrained by the requirements of bail mechanism. The present bail mechanism, in Skyhook IV, requires a cable tension of 30 pounds. This is in spite of the fact that this prototype is not designed to fly in wind velocities higher than 40 feet/second. A high tension is undesirable for reasons mentioned later in this section. Moreover, since the bail is to be torqued at

the upper end, the effective cable junction is therefore constrained to be at the lower end of the bail, which in Skyhook IV is six feet below the centre of gravity of the periscopter platform.

Cable Tension: An increase in cable tension means an increase in thrust required, or a penalty in the weight of the periscopter. An increase in the thrust is accompanied by an increase in power. Thrust can be increased in two ways only. Either the collective pitch setting θ_c is to be increased. This results in reduced control power available in the rigid feathering rotor. Alternatively, the constant Y ($= \frac{1}{8}\rho a C_o \Omega^2 R^3$) is to be increased. This increases Y_M; and hence the unbalanced moments. This would be undersirable if the bail mechanism is used for control. The value of the feathering angles required to balance the unbalanced moments are, however, not affected. Moreover, an increase in thrust is accompanied by an increase in induced velocity. An increase in induced velocity increases unbalanced moments, and also the feathering angle A required to balance the unbalanced pitch moment ($A \backsim K\lambda_{o1}$). Thus the considerations of power required, the control power available, the unbalanced moments produced and also the strength of the cable itself, lead to a low value of the cable tension. In section 4.3 it was shown (for the case of zero wind flights) that the low value of the cable tension surpresses the undesirable flying characteristics at low altitudes and for positive values of ℓ_2. In fact, a zero cable tension results in static stability, elimination of positional controls, elimination of the divergent mode for all values of ℓ_2. (No results have been obtained for non-zero wind

conditions. But at least for low wind conditions one can expect similar results).

The analysis developed in Section 4.3 should enable one to compute the stability characteristics of the periscopter for all wind conditions. The analysis is not limited to periscopters using rigid feathering rotor systems. For zero winds, the stability characteristics have been obtained analytically. The results show that, without controls, the periscopter is always dynamically unstable. Static stability can be obtained by attaching the cable at a point above the centre of gravity of the periscopter. Dynamic and static stability can be obtained by the use of controls. It should be possible to achieve inherent stability by coupling the swash plate to suitable gyros. It is interesting to note that the controls involve all the three parameters, i.e., ℓ_1, ℓ_2 and P_o, which distinguish a periscopter from a helicopter. The analysis also reveals a possible cause for the poor flying qualities of the test models: this is the rapid divergent mode, appearing at low flight altitude, high tension and positive ℓ_2.

6. SELECTED BIBLIOGRAPHY

(1) Amer, K.B. "Means for achieving desirable handling characteristics in a small helicopter", American Helicopter Society Annual Forum, 1959, pages 77-84.

(2) Castles, Jr. Walter, and De Leeuw, Jacob Henri, "The normal component of the induced velocity in the vicinity of a lifting rotor and some examples of its application", NACA Technical Note 2912, March 1953.

(3) Clarke, A.E. and Bramwell, A.R.S., "Selected aspects of the aerodynamics of rotorcraft", The Aeronautical Journal of Royal Aeronautical Society, Volume 72, February 1968, pages 178-186.

(4) Collar, A.R., "The design of contra-rotating fans", Journal of the Royal Aeronautical Society, Volume 67, November 1968, pages 725-730.

(5) Coleman, Robert, P., Feingold, Arnold, M., and Stempin, Carl, W., "Evaluation of the induced-velocity field of an idealised helicopter rotor", NACA - ARR L5EIO.

(6) Cresap, W.L., "Rigid rotor development and flight tests", Institute of the Aeronautical Sciences paper No. 26-17, January 1962.

(7) Culver, L.I., "Progress on Rigid Rotor Concept", The Journal of the Royal Aeronautical Society", Volume 72, February 1968, pages 187-190.

(8) Curtiss, H.C., and Seckel, E., "Helicopter rotor forces and moments", Princeton University Aeronautical Engineering Report 659, 1968.

(9) Focke, E.H., "German thinking on rotary-wing development", Journal of the Royal Aeronautical Society, Volume 69, May 1965, pages 293-305.

(10) Gessow, Alfred, and Myers, Jr., Garry C., "Aerodynamics of the helicopters", Frederick Ungar Publishing Co., New York, 1952.

(11) Gessow, Alfred, "Review of information on induced flow of a lifting rotor", NACA Technical Note 3238, August 1954.

(12) Glauert, H., "The elements of aerofoil and airscrew theory", Cambrige University Press, London, 1959.

(13) Gustafson, F.B., and Tabscott, Robert J., "Methods for obtaining desired helicopter stability characteristics and procedures for stability predictions", NACA Report 1350, 1958.

(14) Heppe, R.R., "The single rotor helicopter with rigidly mounted blades", Journal of the Royal Aeronautical Society, Volume 67, October 1963, pages 651-663.

(15) McCormick, Jr., Barnes W., "Aerodynamics of V/STOL flight", Academic Press, New York, 1967.

(16) Mangler, K.W., and Squire, H.B., "The induced velocity field of a rotor", Reports and Memoranda No. 2642, 1953.

(17) Miller, R.H., "Helicopter control and stability in hovering flight", Journal of the Royal Aeronautical Sciences, Volume 15, No. 8, August 1948, Pages 453-472.

(18) Payne, P.R., "Helicopter stability in hovering flight", Journal of the Royal Aeronautical Society, Volume 59, September 1955, pages 635-640.

(19) Payne, P.R., "High offset flapping pin rotor analysis", Aircraft Engineering November 1954, pages 378-382.

(20) Payne, P.R., "Helicopter dynamics and aerodynamics", Sir Isaac Pitman & Sons Ltd., London, 1959.

(21) Poole, J., "Rotorcraft work at the aeroplane and armament experimental establishment", Journal of the Royal Aeronautical Society, Volume 67, August 1968, pages 501-513.

(22) Price, H.L., "Rotor dynamics and helicopter stability", Aircraft Engineering, March 1963.

(23) Seckel, Edward, "Stability and control of airplanes and helicopters", Academic Press, New York, 1964.

(24) Statler, W.H., Heppe, R.R. and Cruz, E.S., "Results of the XH-SIA rigid rotor research helicopter program", American Helicopter Society Annual Forum, 1963, pages 119-133.

(25) Stuart III Joseph, "The Helicopter control rotor, Volume 7, No. 8, August 1948, pages 33-37.

(26) Tararine, S., "Experimental and theoretical study of local induced velocities over a rotor disc", CAL/TRECOM Symposium Proceeding on "Dynamic load problems associated with helicopters and V/STOL A/C", Volume I, June 26-28, Buffalo, New York.

(27) Willmer, M.A.P., "The loading of helicopter rotor blades in forward flight", Report and Memoranda No. 3318, 1963.

APPENDIX 1

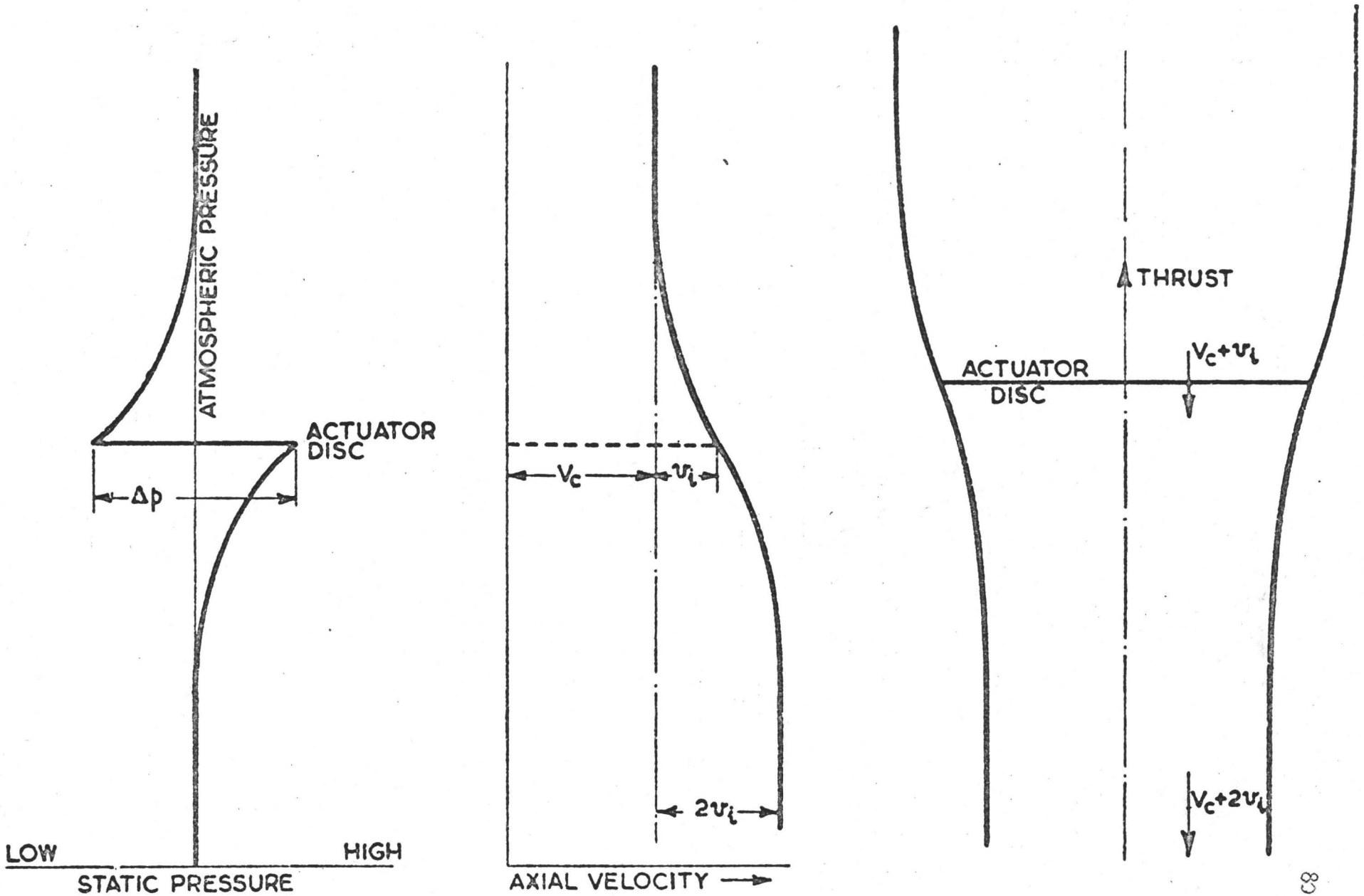
ATMOSPHERIC PRESSURE
ACTUATOR DISC
Δp
LOW
HIGH
STATIC PRESSURE
V_c
v_i
$2v_i$
AXIAL VELOCITY
THRUST
ACTUATOR DISC
V_c+v_i
V_c+2v_i

FIGURE I

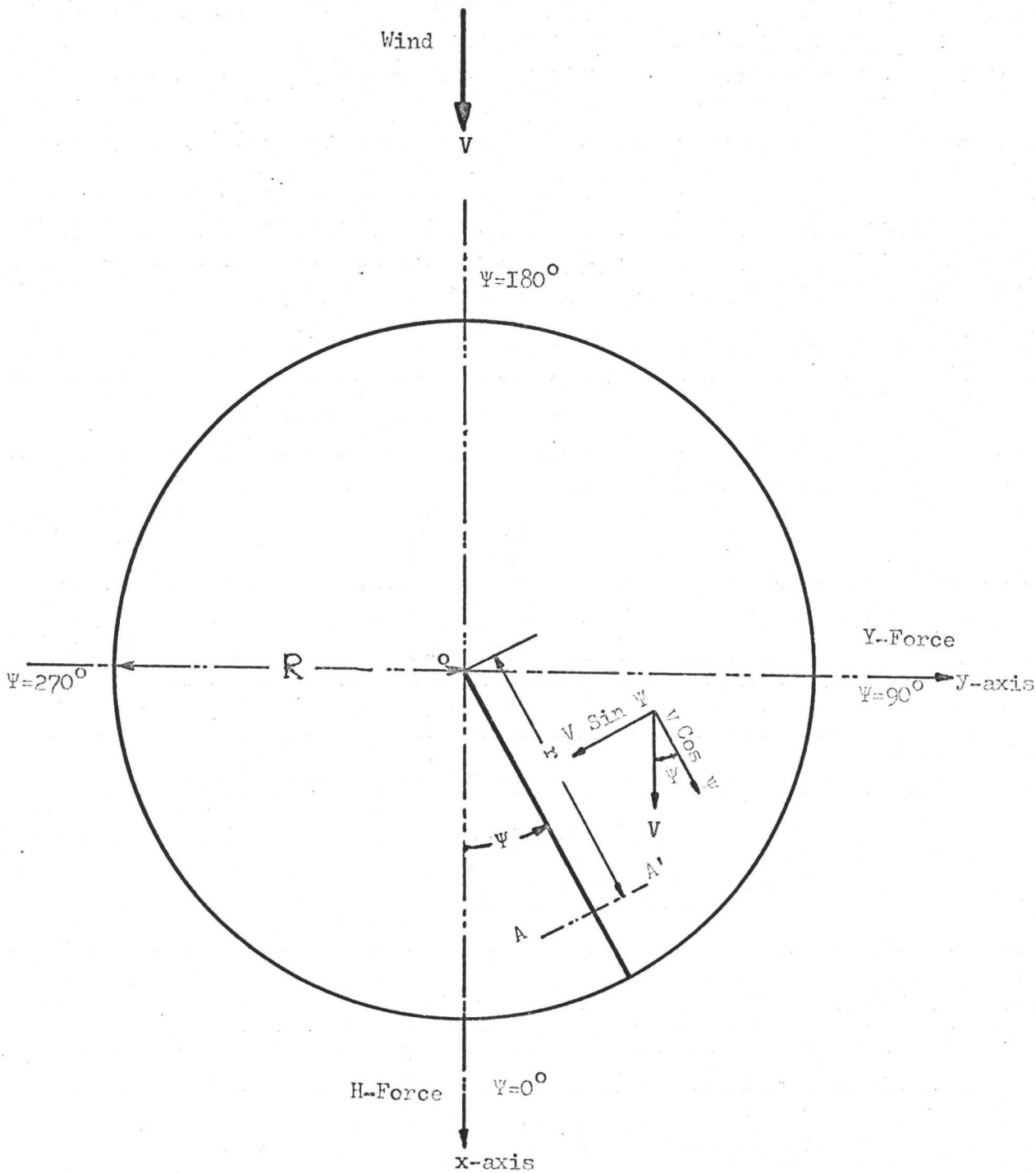

Plan View of a Lifting Rotor

FIGURE 2

Airflow at an Elemental Section AA' of Blade

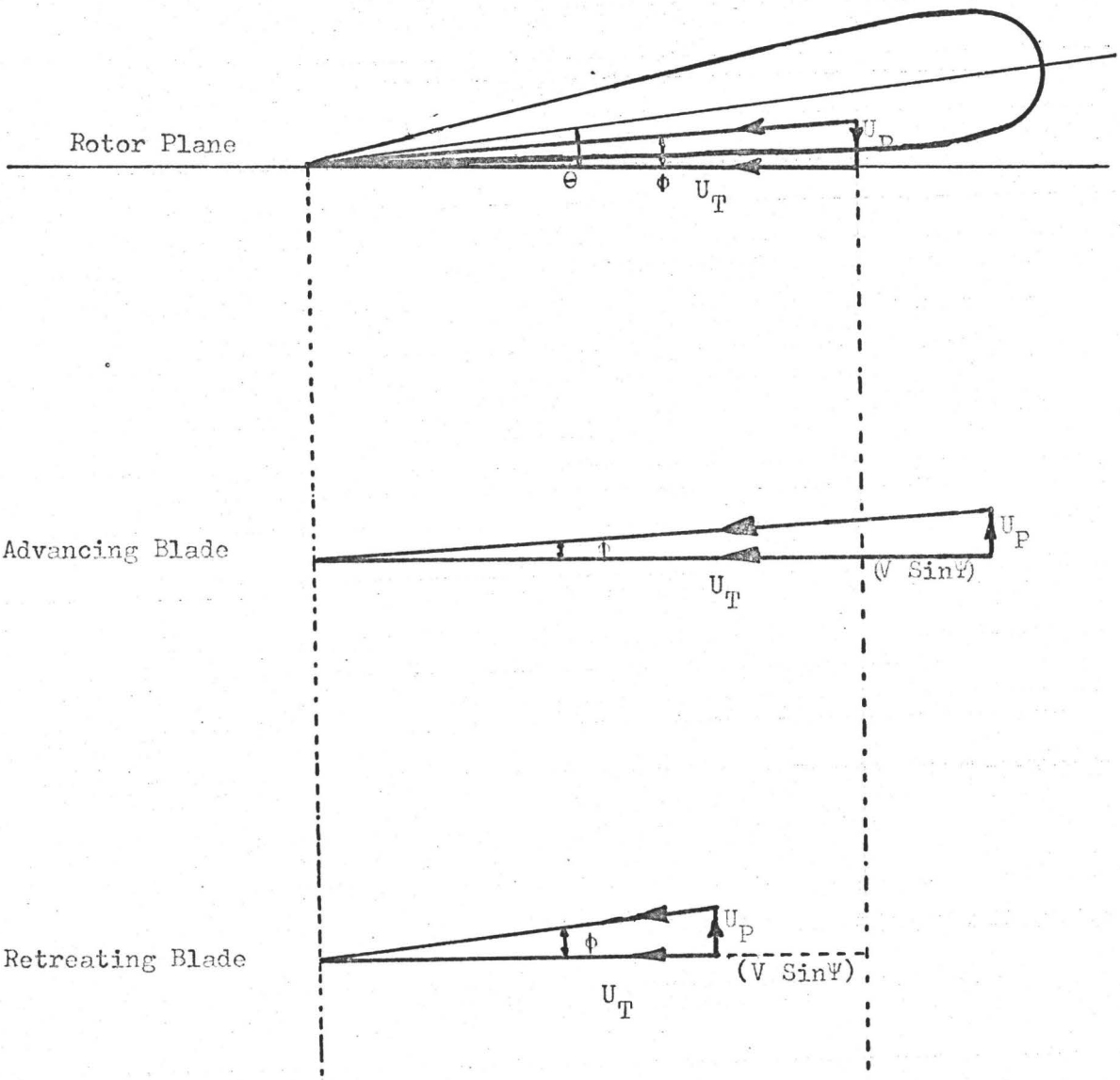

FIGURE 3

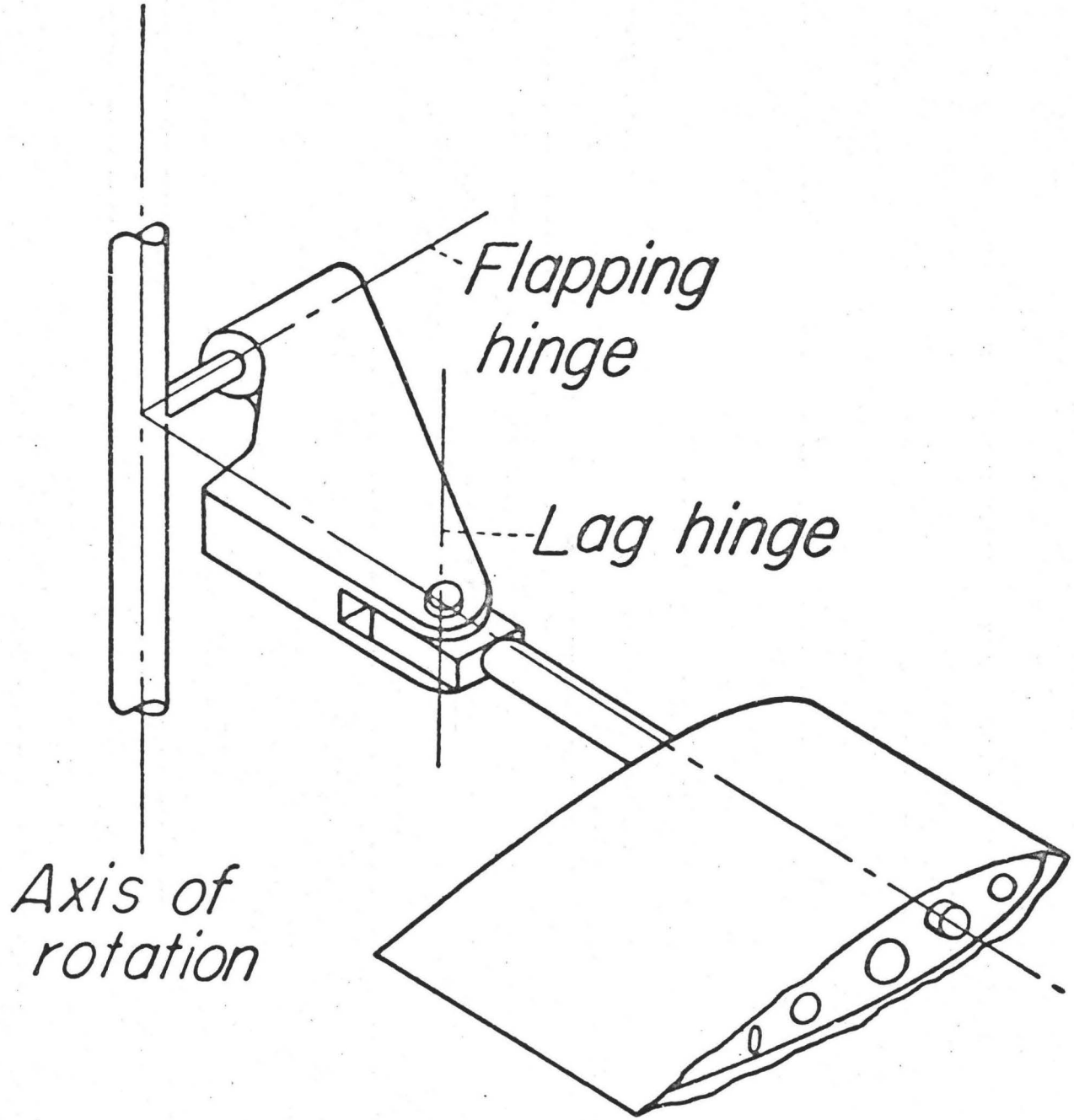

Flapping Rotor

FIGURE 4

Forces on a Flapping Blade

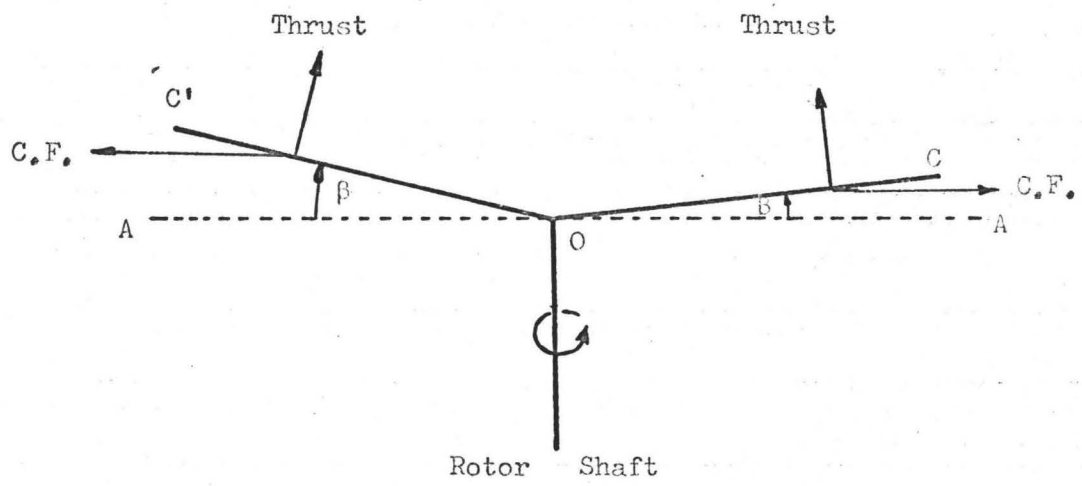

FIGURE 5

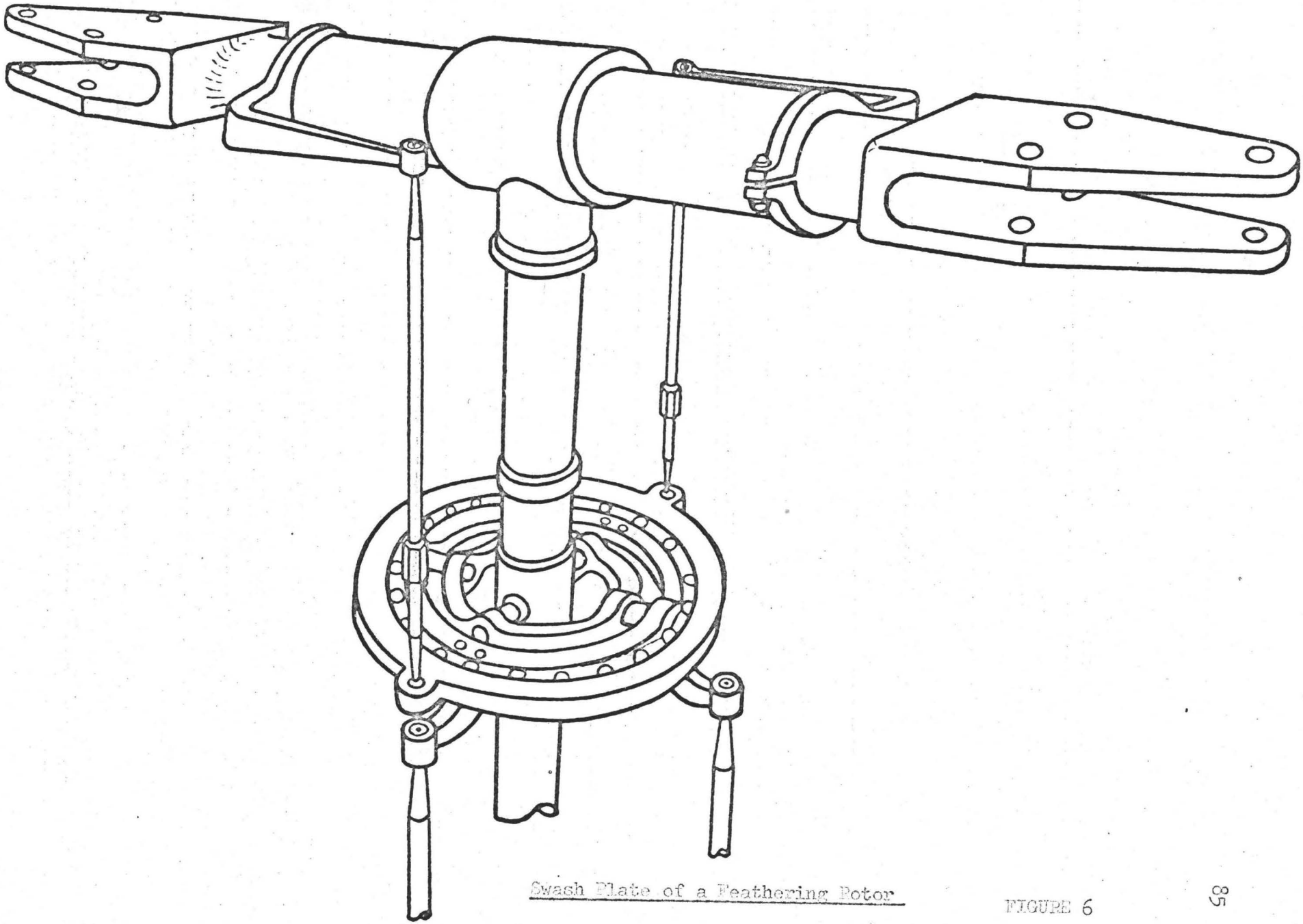

Swash Plate of a Feathering Rotor

FIGURE 6

Induced Velocity over Blade Span in Still Air

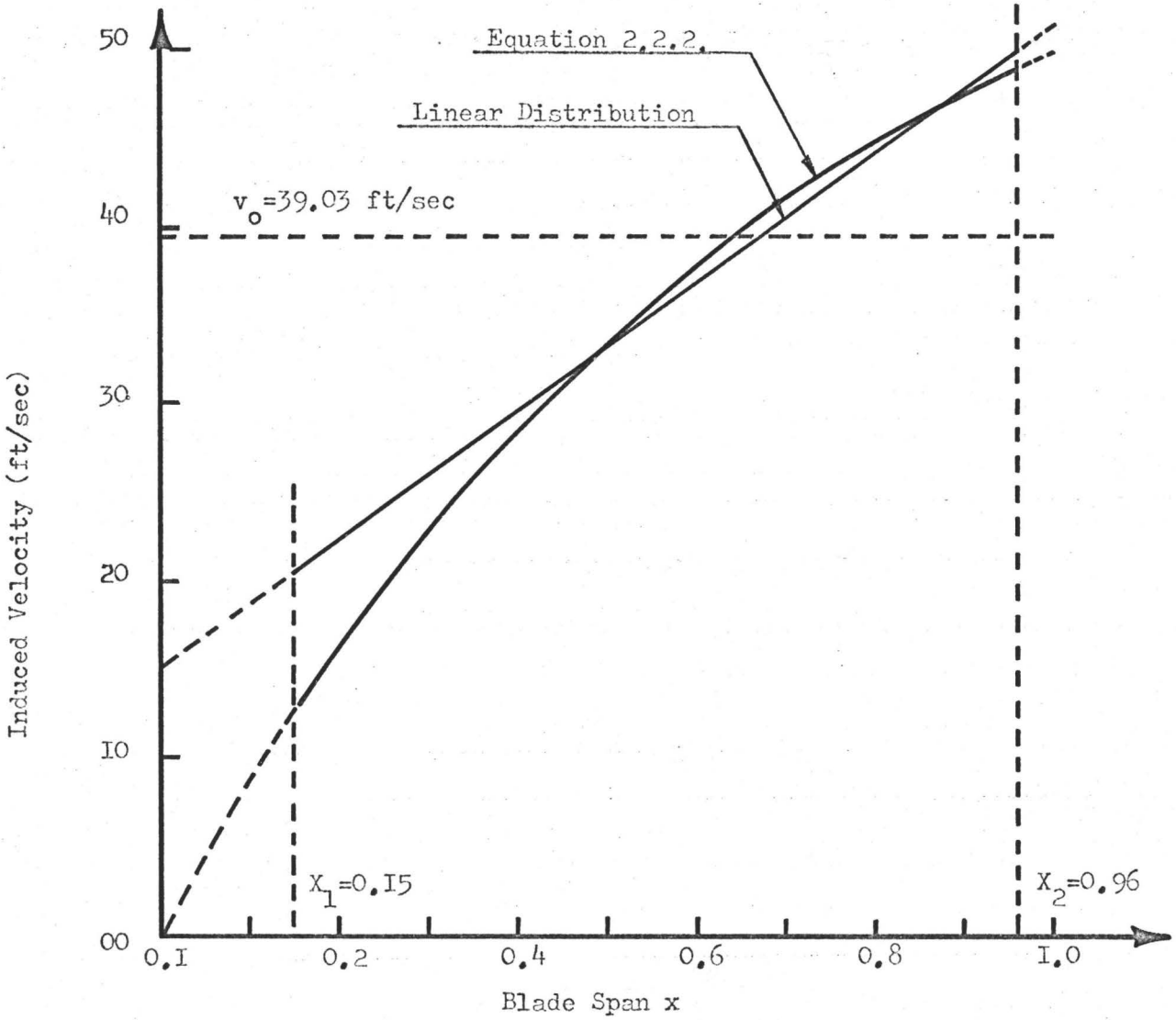

FIGURE 7

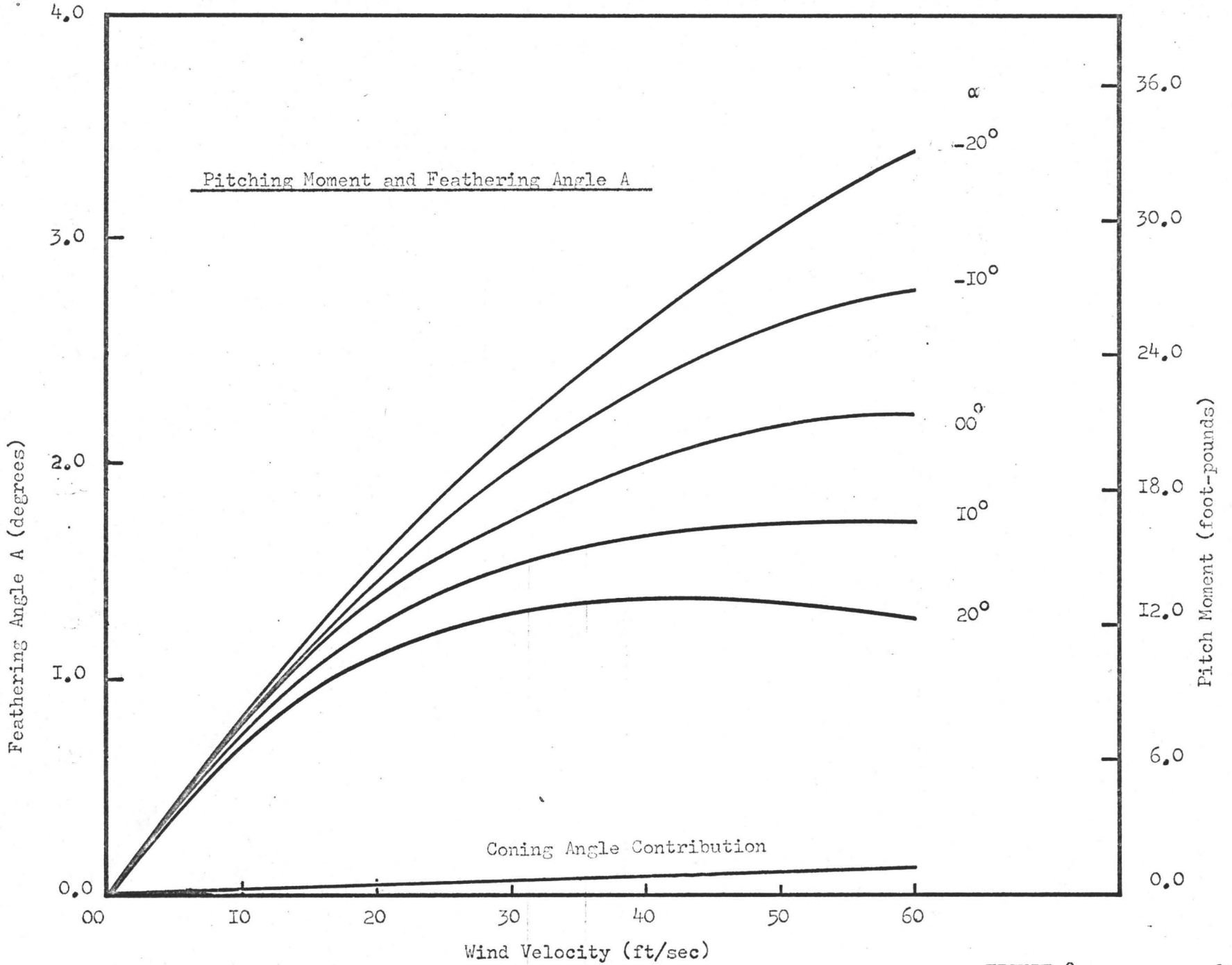
Pitching Moment and Feathering Angle A
α
-20°
-10°
0°
10°
20°
Coning Angle Contribution
Feathering Angle A (degrees)
Pitch Moment (foot-pounds)
Wind Velocity (ft/sec)
4.0
3.0
2.0
1.0
0.0
36.0
30.0
24.0
18.0
12.0
6.0
0.0
00
10
20
30
40
50
60

FIGURE 8

FORTRAN PROGRAM

```
C       INDUCED VELOCITY DISTRIBUTION IN STILL AIR
C
C       ROTOR DATA
        R=26.0/12.0
        N=314
        CR=51.0/(16.0*12.0)
        TR=R/(20.0*CR)
        P=0.149
        X1=0.15
        X2=0.96
        X3=1.0
        B=4.0
        A=6.0
        DRCOEF=0.007
        RO=0.002378
        VC=0.0
C
        PIE=22.0/7.0
        RADIAN=180.0/PIE
        Q=N
        X=0.0
2       CONTINUE
        S=B*CR*(1.0-TR*X)/(R*PIE)
        AA=S*A*Q*R/16.0
        AB=AA+VC/2.0
        BB=(4.0*VC*VC/(16.0*AA))+VC+AA
        CC=2.0*((P*X*Q*R)-VC)/BB
        VIC=AB*(-1.0+SQRT(1.0+CC))
        WRITE(6,41)  X,VIC
        X=X+0.1
        IF(X.GT.1.0) GO TO 1
        GO TO 2
41      FORMAT(10X,2HX=,F4.2,10X,17HINDUCED VELOCITY=,F10.3/)
1       CONTINUE
        STOP
        END
```

CD TOT 0036

FORTRAN PROGRAM

```
C       CALCULATION FOR INDUCED VELOCITY, THRUST, H.P, MOMENTS,
C         FEATHERING ANGLES, ANGLE OF ATTACT
        DIMENSION AA(9), XX(9), CC(9) , T(9),T2(9),ATT(9) ,SAT(9),AM(9)
C
C       ROTOR DATA
        R=26.0/12.0
        N=314
        CR=51.0/(16.0*12.0)
        TR=R/(20.0*CR)
        P=0.149
        X1=0.15
        X2=0.96
        X3=1.0
        B=4.0
        A=6.0
        DRCOEF=0.007
        RO=0.002378
        G=36.0
        H=15.0
        FA=0.0
        FB=0.0
C
C       PRELIMINARY CALCULATIONS
        PIE=22.0/7.0
        RADIAN=180.0/PIE
        S=N
        TIP=(X2**2.0-X1**2.0)
        Y=RO*A*CR*S**2.0*R**3.0*B/8.0
        YY=R*S
        YM=0.25*R*Y
        YYY=(Y/(2.0*RO*PIE*R*R*YY*YY*TIP))**2.0
        WRITE(6,11)Y, YY, YM,  YYY
C       TAPER INTEGRALS
        DO 1 M=1,5
        D=M
        T(M)=4.*((X2**D-X1**D)/D)-4.*TR*(X2**(D+1.)-X1**(D+1.))/(D+1.)
        T2(M)=4.*((X3**D-X1**D)/D)-4.*TR*(X3**(D+1.)-X1**(D+1.))/(D+1.)
        WRITE(6,12) D,T(M)
1       CONTINUE
        WRITE(6,13)
```

CD TOT 0040

```
C       VARY THE WIND VELOCITY FROM 0.0 TO 60.0 F.P.S.
        DO 5 J=1,40
        Z=J
        STEP=10.0
        V=-STEP
        V=V+STEP*Z
C       VARY THE DIRECTION OF WIND FROM -20TO +20 DEGREES
        DO3 JJ=1,40
        ZZ=JJ
        STEPAL=PIE/18.0
        AL=-3.0*STEPAL
        AL=AL+ZZ*STEPAL
C
C       INDUCED VELOCITY
        U=V*COS(AL)/YY
        DC2=(V*SIN(AL))/YY
        XY=P*T(3)+.5*U*U*T(1)*P-T(2)*DC2-FB*U*T(2)
        NN=4
        AA(1)=1.0
        AA(2)=2.0*DC2
        AA(3)=(DC2*DC2+U*U-YYY*T(2)*T(2))
        AA(4)=2.0*XY*YYY*T(2)
        AA(5)=-YYY*XY*XY
        IF(J.EQ.1) GO TO 2
        CALL BAIRST (AA,XX,CC,NN)
        GO TO 7
2       CONTINUE
        IF(JJ.GT.1) GO TO 4
        G=G/YY
        H=H/YY
        CT=P*T(3)-G*T(3)-H*T(2)
        THRUST=CT*Y
        YAY=SQRT(YYY)
        XX(1)=(-YAY*T(2)+SQRT((YAY*T(2))**2+4.*YAY*XY))/2.0
        DC1=XX(1)
        DC=DC1
        WRITE(6,15) THRUST
        AL=0.0
        RM =0.0
        ATT(2)=0.0
        CMR=0.0
        CMPVK=0.0
        ACON =0.0
        GO TO 63
7       CONTINUE
C       POSITIVE REAL ROOT GIVES THE INDUCED VELOCITY
        DC1=XX(1)
        IF(CC(1).GT.0.0) GO TO 61
        GO TO 62
61      DC1=XX(3)
62      CONTINUE
        DC=DC1+DC2
```

CD TOT 0052

```
C     K-FACTOR FOR LINEAR VARIATION OF INDUCED VELOCITY
      UDC=U/DC
      VK=(1.333*UDC)/(1.2+UDC)
      VKVSVO=-(3.6*VK*DC1)/(4.0*U)
C
C     THRUST
   63 CONTINUE
      CT=(P*T(3)+P*U*U*T(1)*0.5-DC*T(2))
      THRUST=CT*Y
      TVSVO=-(T(2)*DC1/CT)
C
C     H.P. REQUIRED
      CQ= CT*DC+DRCOEF*(T2(4)+0.5*T2(2)*U*U)/A
      HP=CQ*YY*Y/550.0
      IF(J.EQ.1) GO TO 8
C
C     ROLLING MOMENT
      CMR=2.0*U*P*T(3)-U*DC*T(2)
      RM=CMR*YM
C
C     PITCHING MOMENT
      FO=1.0/RADIAN
      CMPCON=FO*U*T(3)
      CMPVK=DC1*VK*T(4)
C
C     FEATHERING  COEFFICIENTS
      FB=RADIAN*CMR/T(4)
      FA=-RADIAN*(DC1*VK)
      ACON= (FO *U*T(3)/T(4))*RADIAN
C
C     BLADE ELEMENTAL ANGLE  OF ATTACK
      X=1.0
      DO 31 L=1,4
      PHI=0.0
      ZL=L
      SIE=-PIE/18.0+PIE*ZL/36.0
      UT=X+U*SIN(SIE)
      UP=DC+FO*U*COS(SIE)+DC1*VK*X*COS(SIE)
      PHI=RADIAN*UP/UT
      ATT(L)=P*RADIAN-PHI-2.0*FA*COS(SIE)
      SAT(L)=P*RADIAN-PHI-1.0*FA*COS(SIE)
      AM(L)=(12.0-ATT(L))
      IF(L.EQ.2) GO TO 32
   31 CONTINUE
   32 CONTINUE
```

```
C
  8      CONTINUE
         PRAD=P*RADIAN
         DC1=DC1*YY
         DAL=AL*RADIAN
         WRITE(6,14) V,DAL,DC1,CT,THRUST,HP, RM,CMPVK,FB,FA,ACON,ATT(2)
         WRITE(7,24)DAL,DC1,CT,THRUST,HP
         WRITE(7,25) DAL,FB,CMPVK, FA, ACON
         WRITE(7,26) DAL ,PHI, ATT(2),SAT(2),AM(2)
         FA=0.0
         FB=0.0
C
         ST=PIE/18.0
         IF(AL.GT.ST) GO TO 4
  3      CONTINUE
  4      CONTINUE
         IF(V.EQ.60.0) GO TO 6
  5      CONTINUE
  6      CONTINUE
 11      FORMAT(18X,2HY=,F10.4,7X,3HYY=,F10.4,7X,3HYM=,F10.4,6X,4HYYY=,
     3   F6.4////)
 12      FORMAT(40X, 2HN=, F4.1, 15X, 15HTAPER INTEGRAL=, F10.6//)
 13      FORMAT(7X,1HV,6X,5HALPHA,4X,2HIV,10X,2HCT,4X,6HTHRUST,7X,3HH.P,
     4   7X,2HRM,10X,3HCMP,12X,1HB,8X,1HA,6X,4HACON,5X,1HI/)
 14      FORMAT(5X,F5.1,3X,F5.1,3X,F6.2,6X,F6.3,3X,F6.2,6X,F6.3,3X,
     5   F6.2,6X,F6.3,4X,F6.2,3X,F6.2,3X,F6.2,3X,F6.2//)
 15      FORMAT(15X,34HTHRUST USING BLADE ELEMENT THEORY=,F6.2)
 25      FORMAT(20X,F6.2,5X,F5.2,5X,F5.3,5X,F5.2,5X,F5.2)
 26      FORMAT(20X,F6.2,5X,F5.2,5X,F5.2,5X,F5.2,5X,F6.2)
         STOP
         END
```

CD TOT 0031

TABLE 1

Thrust using blade elemental theory(in still air) = 96.1 pounds

Power using blade elemental theory(in still air) = 8.66 hp.

α	v_o(ft/sec)	C_T	T(pounds)	h.p.
WIND VELOCITY=00.0 FT/SEC.				
0.00	38.43	.049	93.16	8.35
WIND VELOCITY=10.0 FT/SEC.				
-20.00	40.55	.052	97.99	8.46
-10.00	39.32	.051	96.35	8.43
0.00	38.07	.050	94.54	8.39
10.00	36.86	.049	92.61	8.35
20.00	35.70	.048	90.64	8.29
WIND VELOCITY=20.0 FT/SEC.				
-20.00	41.98	.056	105.54	8.59
-10.00	39.50	.054	102.31	8.55
0.00	37.06	.052	98.48	8.48
10.00	34.74	.050	94.23	8.40
20.00	32.58	.047	89.76	8.28
WIND VELOCITY=30.0 FT/SEC.				
-20.00	42.71	.061	115.81	8.68
-10.00	39.06	.058	110.70	8.66
0.00	35.56	.055	104.39	8.60
10.00	32.29	.051	97.24	8.48
20.00	29.27	.047	89.67	8.30
WIND VELOCITY=40.0 FT/SEC.				
-20.00	42.82	.068	128.47	8.66
-10.00	38.15	.064	120.96	8.72
0.00	33.77	.059	111.53	8.70
10.00	29.71	.053	100.86	8.58
20.00	25.99	.047	89.62	8.32
WIND VELOCITY=50.0 FT/SEC.				
-20.00	42.46	.075	143.01	8.45
-10.00	36.96	.070	132.41	8.66
0.00	31.87	.063	119.22	8.77
10.00	27.18	.055	104.45	8.67
20.00	22.88	.047	89.08	8.33
WIND VELOCITY=60.0 FT/SEC.				
-20.00	41.79	.084	158.84	8.00
-10.00	35.65	.076	144.48	8.49
0.00	30.00	.067	126.96	8.79
10.00	24.80	.057	107.63	8.75
20.00	20.03	.046	87.75	8.33

TABLE 2

Moments and Feathering Angles

α°	B° *	C_{MP}	A° **	$ACON^{\circ}$
WIND VELOCITY=00.0 FT/SEC.				
0.00	0.00	0 000	0.00	0.00
WIND VELOCITY=10.0 FT/SEC.				
-20.00	.24	.008	-.79	.02
-10.00	.25	.008	-.79	.02
0.00	.25	.008	-.77	.02
10.00	.24	.007	-.73	.02
20.00	.23	.007	-.67	.02
WIND VELOCITY=20.0 FT/SEC.				
-20.00	.49	.015	-1.45	.04
-10.00	.50	.014	-1.39	.04
0.00	.51	.013	-1.29	.04
10.00	.49	.012	-1.17	.04
20.00	.46	.011	-1.04	.04
WIND VELOCITY=30.0 FT/SEC.				
-20.00	.75	.020	-2.01	.06
-10.00	.77	.019	-1.85	.06
0.00	.77	.017	-1.65	.06
10.00	.74	.015	-1.44	.06
20.00	.69	.012	-1.22	.06
WIND VELOCITY=40.0 FT/SEC.				
-20.00	1.03	.025	-2.49	.08
-10.00	1.06	.022	-2.19	.08
0.00	1.05	.019	-1.88	.08
10.00	1.00	.016	-1.58	.08
20.00	.92	.013	-1.29	.08
WIND VELOCITY=50.0 FT/SEC.				
-20.00	1.34	.029	-2.89	.10
-10.00	1.37	.025	-2.46	.10
0.00	1.34	.021	-2.03	.10
10.00	1.26	.017	-1.63	.10
20.00	1.15	.013	-1.27	.10
WIND VELOCITY=60.0 FT/SEC.				
-20.00	1.68	.033	-3.23	.12
-10.00	1.69	.027	-2.65	.12
0.00	1.64	.021	-2.10	.13
20.00	1.37	.012	-1.21	.12
10.00	1.53	.017	-1.62	.12

* Rolling Moment = $Y_M t_4 B$ foot pounds

** Pitching Moment= $Y_M t_4 A$ foot pounds

TABLE 3

Angle of Incidence

α^o	ϕ^o	i^{o*}	i^{o**}	A_m
WIND VELOCITY=00.0 FT/SEC.				
0.0	3.51	5.00	5.00	7.00
WIND VELOCITY=10.0 FT/SEC.				
-20.00	3.93	6.19	5.39	5.81
-10.00	3.97	6.15	5.36	5.85
0.00	3.99	6.08	5.31	5.92
10.00	3.99	6.00	5.27	6.00
20.00	3.98	5.89	5.23	6.11
WIND VELOCITY=20.0 FT/SEC.				
-20.00	4.44	7.00	5.55	5.00
-10.00	4.45	6.86	5.47	5.14
0.00	4.44	6.67	5.38	5.33
10.00	4.42	6.46	5.29	5.54
20.00	4.39	6.23	5.19	5.77
WIND VELOCITY=30.0 FT/SEC.				
-20.00	4.79	7.77	5.76	4.23
-10.00	4.74	7.49	5.64	4.51
0.00	4.69	7.14	5.50	4.86
10.00	4.64	6.77	5.33	5.23
20.00	4.59	6.39	5.16	5.61
WIND VELOCITY=40.0 FT/SEC.				
-20.00	5.00	8.52	6.03	3.48
-10.00	4.88	8.04	5.85	3.96
0.00	4.78	7.51	5.63	4.49
10.00	4.72	6.96	5.39	5.04
20.00	4.68	6.42	5.14	5.58
WIND VELOCITY=50.0 FT/SEC.				
-20.00	5.10	9.22	6.33	2.78
-10.00	4.91	8.54	6.08	3.46
0.00	4.78	7.80	5.78	4.20
10.00	4.72	7.07	5.44	4.93
20.00	4.71	6.37	5.10	5.63
WIND VELOCITY=60.0 FT/SEC.				
-20.00	5.10	9.89	6.66	2.11
-10.00	4.86	8.97	6.32	3.03
0.00	4.72	8.02	5.92	3.98
10.00	4.67	7.10	5.48	4.90
20.00	4.70	6.24	5.04	5.76

* With only one rotor feathering

** With both rotors feathering

APPENDIX 2

Forces and Moments on a Periscopter

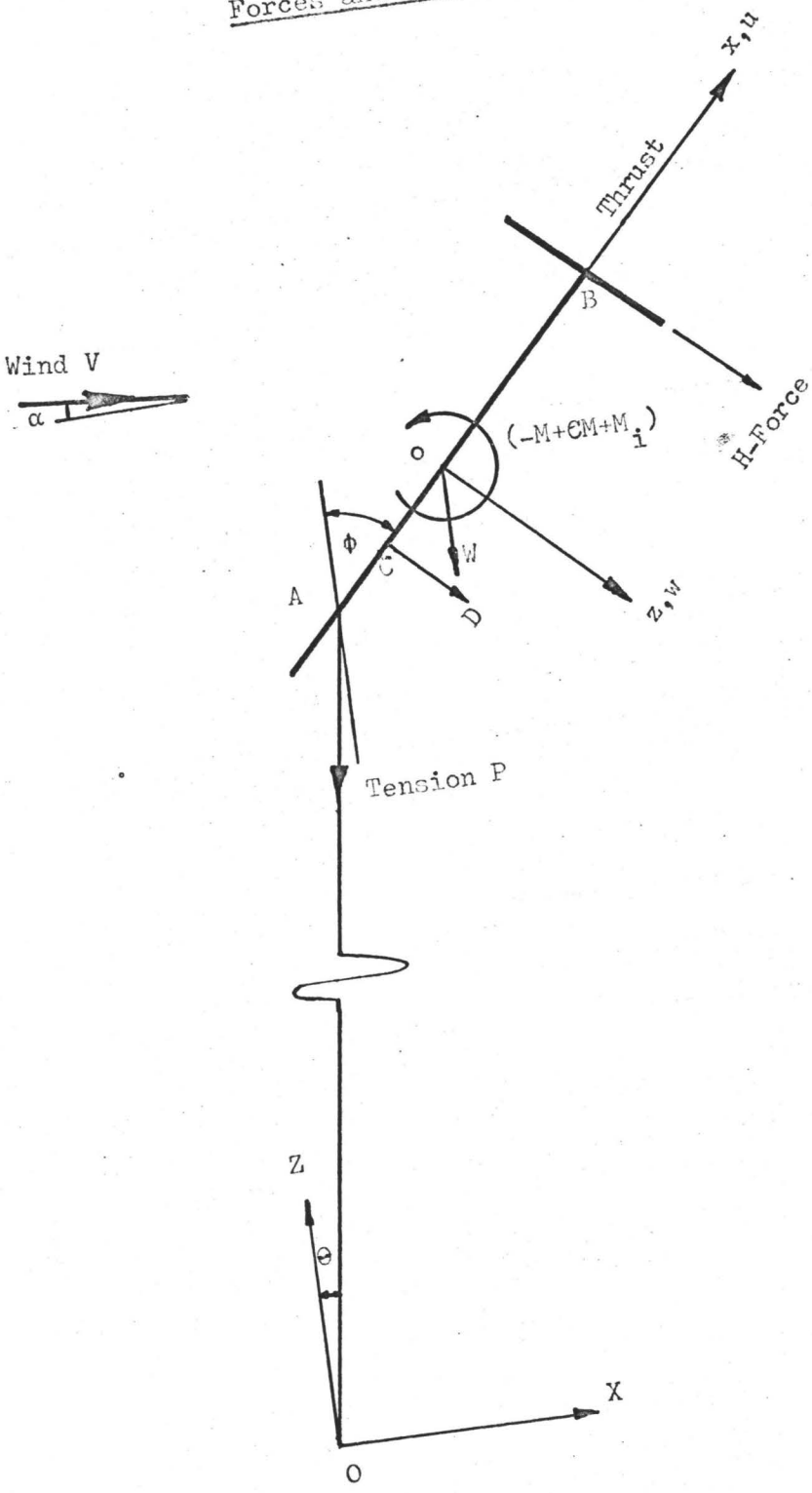

$OA = \ell_1$

$oA = \ell_2$

$oB = \ell_3$

$oC = \ell_4$

FIGURE 9

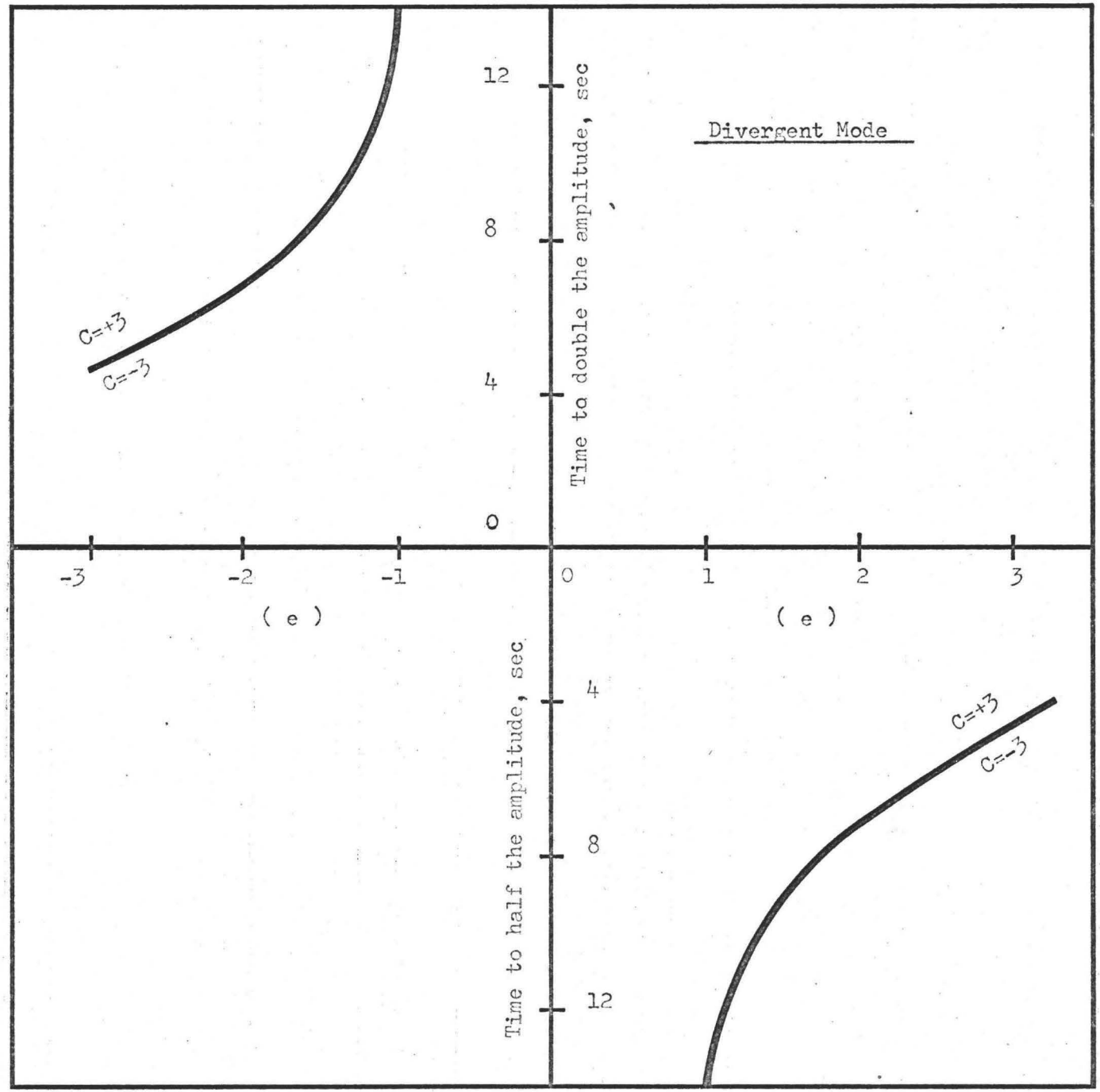
Divergent Mode
Time to double the amplitude, sec
12
8
4
0
C=+3
C=-3
-3
-2
-1
(e)
0
1
2
3
(e)
Time to half the amplitude, sec
4
8
12
C=+3
C=-3

FIGURE 10

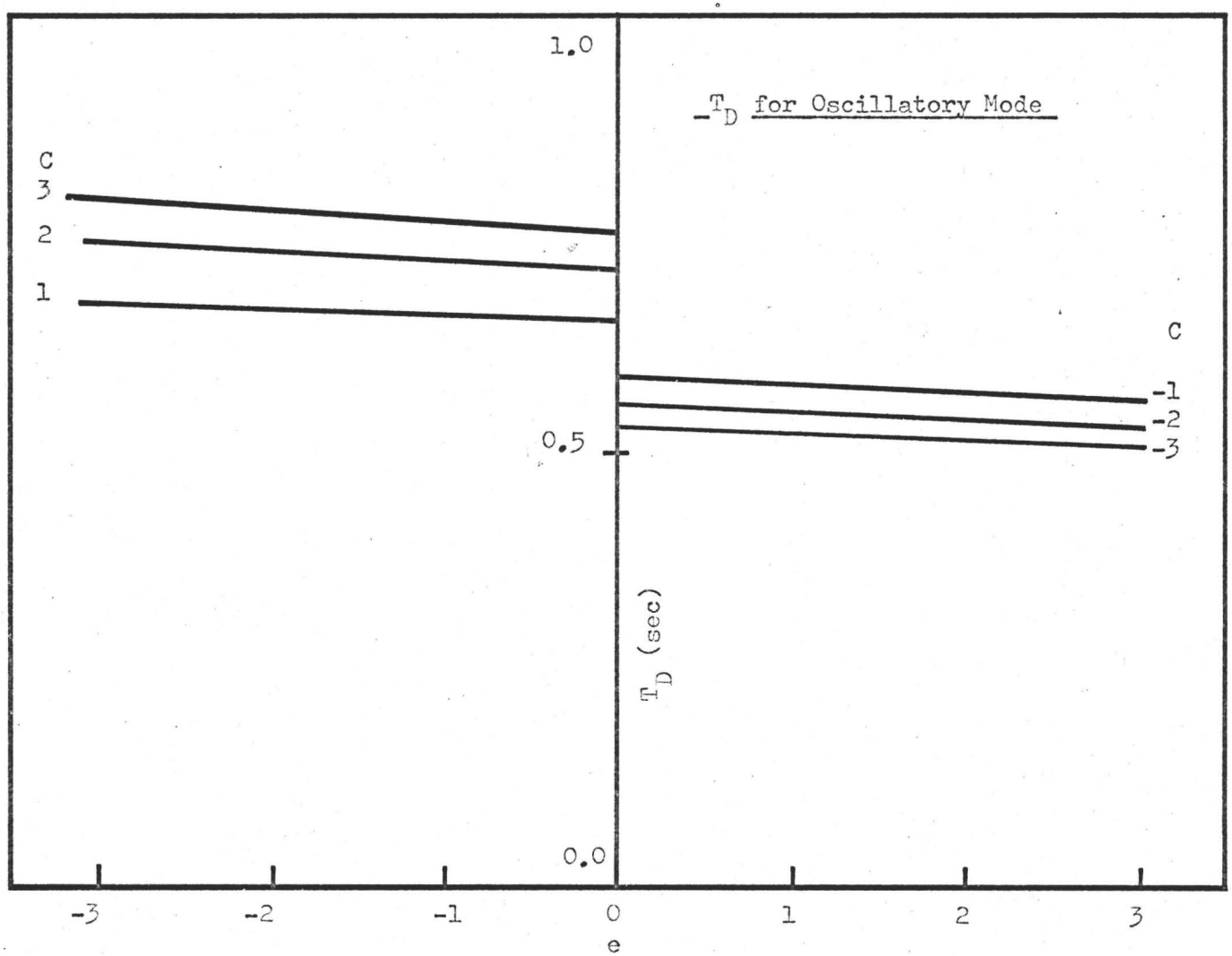

FIGURE 11

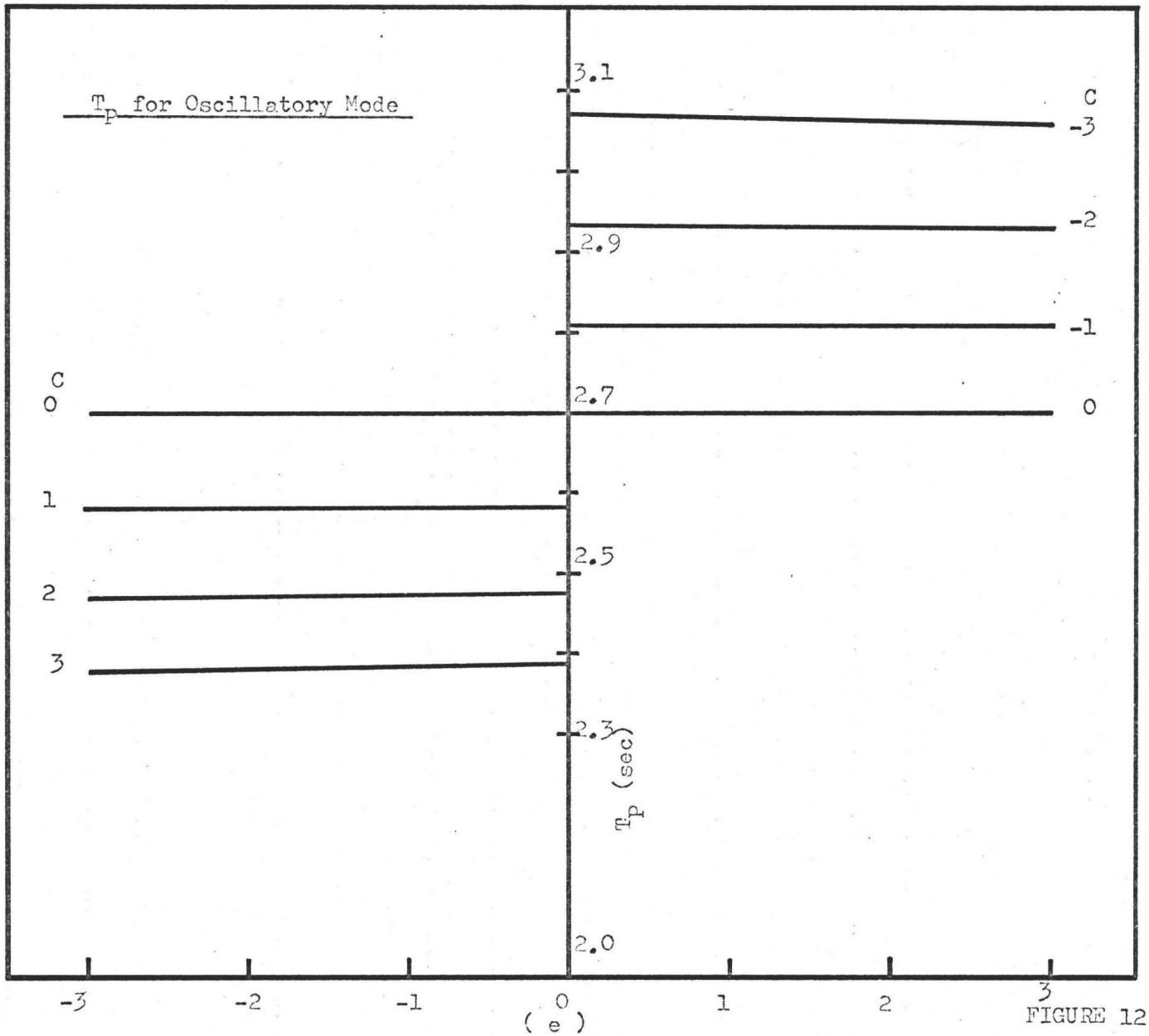

FIGURE 12

McMASTER UNIVERSITY LIBRARY

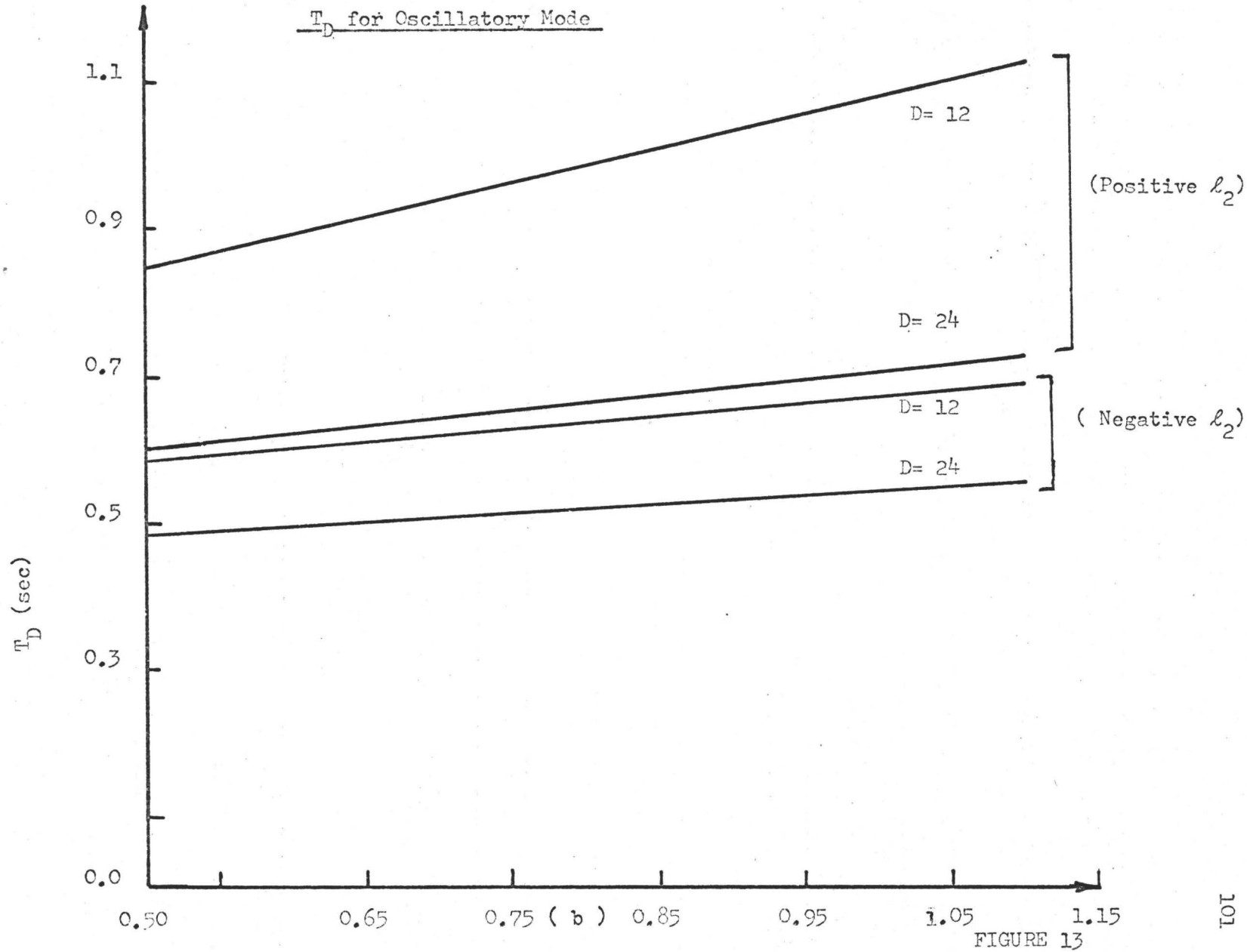
T_D for Oscillatory Mode
1.1
0.9
0.7
0.5
0.3
0.0
T_D (sec)
D= 12
D= 24
D= 12
D= 24
(Positive ℓ_2)
(Negative ℓ_2)
0.50
0.65
0.75 (b)
0.85
0.95
1.05
1.15

FIGURE 13

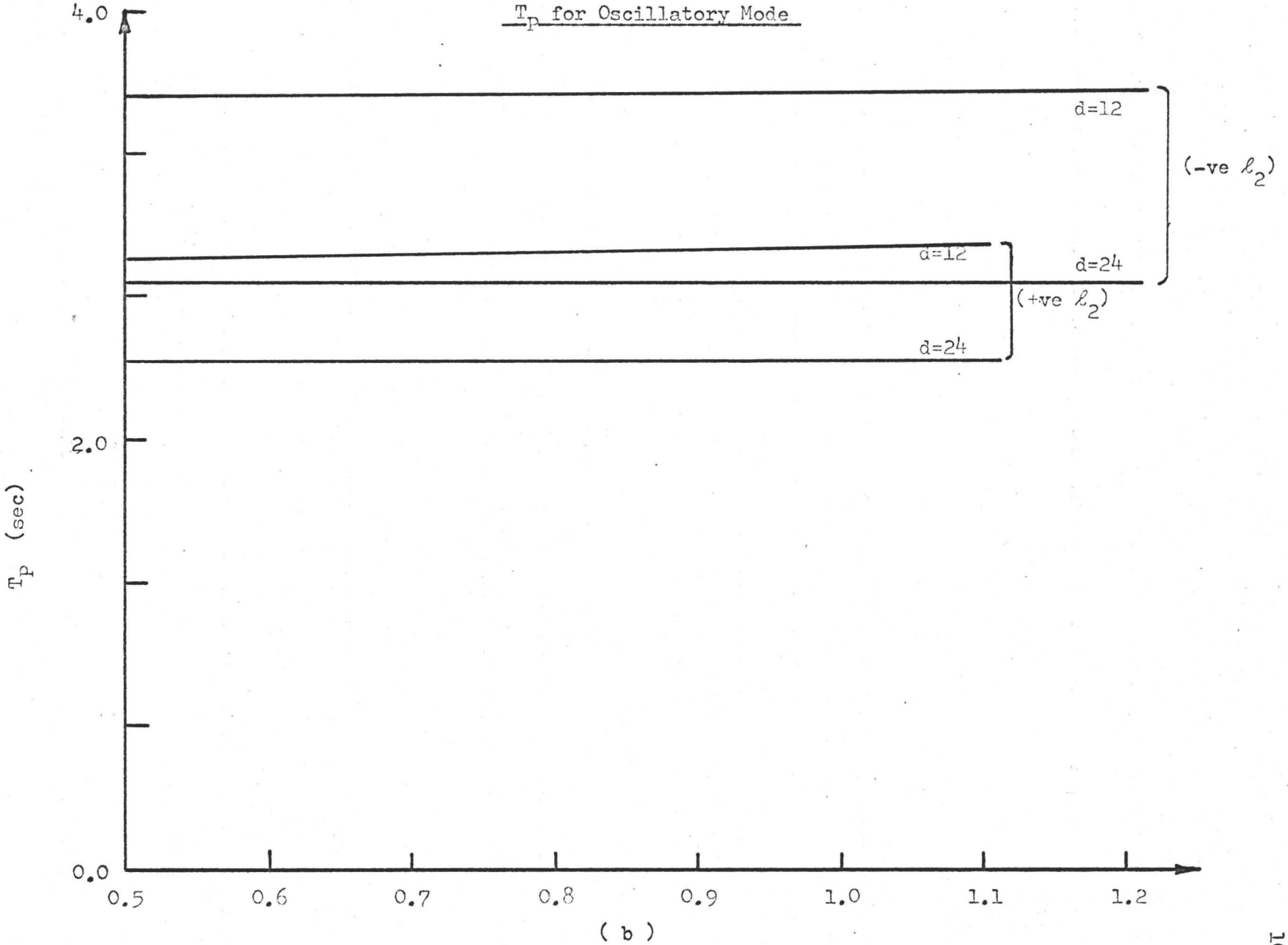
T_p for Oscillatory Mode
4.0
2.0
0.0
T_p (sec)
d=12
(-ve ℓ_2)
d=12
d=24
(+ve ℓ_2)
d=24
0.5
0.6
0.7
0.8
0.9
1.0
1.1
1.2
(b)

FIGURE 14

APPENDIX 2

2.1 Evaluation of Stability Derivatives

Various stability derivatives are evaluated at the trim conditions

$$\theta = \phi = 0$$

and

$$\dot{\theta} = \dot{\phi} = 0 \, .$$

One obtains

$$= \frac{V \cos \alpha - \omega + q \ell_3}{\Omega R}$$

$$= \frac{V \cos \alpha - \ell_1 \dot{\theta} \cos \gamma - \ell_2 \dot{\phi} - \dot{\phi} \ell_3}{\Omega R}$$

The derivatives are

$$\begin{aligned}
\dot{\theta} \quad &= - \frac{\ell_1 \cos \gamma}{\Omega R} \quad = - \frac{\ell_1}{\Omega R} \\
\dot{\phi} \quad &= - \frac{\ell_2 + \ell_3}{\Omega R} \quad = - \frac{\ell_2 + \ell_3}{\Omega R} \\
\theta \quad &= - \frac{\ell_1 \dot{\theta} \sin \gamma}{\Omega R} \quad = 0 \\
\phi \quad &= - \frac{V \sin \alpha \cdot \frac{d\alpha}{d\phi} + \ell_1 \dot{\theta} \sin \alpha}{\Omega R} \quad = - \frac{V \sin \alpha}{\Omega R} \, .
\end{aligned} \tag{1}$$

Also

$$\lambda_{o2} = \frac{V \sin \alpha + u}{\Omega R} = \frac{V \sin \alpha + \ell_1 \dot{\theta} \sin \gamma}{\Omega R}$$

$$\lambda_{o2} \dot{\theta} = \frac{\ell_1 \sin \gamma}{\Omega R} \qquad = 0$$

$$\lambda_{o2} \dot{\phi} = \quad 0 \qquad = 0$$

$$\lambda_{o2\,\theta} = -\frac{\ell_1 \dot{\theta} \cos\gamma}{\Omega R} = 0 \qquad (2)$$

$$\lambda_{o2\,\phi} = \frac{V\cos\alpha + \ell_1 \dot{\theta}\cos\gamma}{\Omega R} = \frac{V\cos\alpha}{\Omega R}\,.$$

Equation 4.1.9 gives for the induced velocity

$$\lambda_{o1}^4 + 2\lambda_{o1}^3 \lambda_{o2} + \lambda_{o1}^2(\mu^2 + \lambda_{o2}^2) = (\text{Constant})\, C_T^{\,2}$$

The derivatives are

$$\lambda_{o1\,\dot{\theta}} = \frac{(\text{Constant})\, C_T C_{T\,\dot{\theta}} - (\lambda_{o1}^3 \lambda_{o2\,\dot{\theta}} + \lambda_{o1}^2(\mu\mu_{\dot{\theta}} + \lambda_{o2}\lambda_{o2\,\dot{\theta}}))}{\lambda_{o1}(2\lambda_{o1}^2 + 3\lambda_{o1}\lambda_{o2} + \mu^2 + \lambda_{o2}^2)}$$

But

$$C_{T\,\dot{\theta}} = (\mu t_1 \theta_c)\,\mu_{\dot{\theta}} - t_2(\lambda_{o1\,\dot{\theta}} + \lambda_{o2\,\dot{\theta}})$$

One obtains, after simplification,

$$\lambda_{o1\,\dot{\theta}} = \frac{(\text{Constant})\, C_T\,(t_1\theta_c\ \mu\mu_{\dot{\theta}})\,(\lambda_{o1}^2\ \mu\mu_{\dot{\theta}})}{\lambda_{o1}(2\lambda_{o1}^2 + 3\lambda_{o1}\lambda_{o2} + \mu^2 + \lambda_{o2}^2) + (\text{Constant})\, t_2 C_T}$$

Similarly,

$$\lambda_{o1\,\dot{\phi}} = \frac{\text{Const}\, C_T\, \theta_c\, \lambda_{o1}^2 \mu^{\,2}\, \mu_{\dot{\phi}}^{\,2}}{\lambda_{o1}(2\lambda_{o1}^2 + 3\lambda_{o1}\lambda_{o2} + \mu^2 + \lambda_{o2}^2) + (\text{Constant})\, C_T t_2}$$

and,

$$\lambda_{o1\,\theta} = 0$$

$$\lambda_{o1\,\phi} = \frac{\text{Const}\, C_T\,(t_1\theta_c\,\lambda_{o2} + t_2)\,\mu^2\,\lambda_{o1}^3}{\lambda_{o1}(2\lambda_{o1}^2 + 3\lambda_{o1}\lambda_{o2} + \mu^2 + \lambda_{o2}^2) + (\text{Constant})\, C_T t_2} \qquad (3)$$

The factor K for longitudinal variation of induced velocity is given by

$$K = \frac{\frac{4}{3}\,\mu/\lambda}{(1.2 + \mu/\lambda)} = \frac{\frac{4}{3}}{(1.2\lambda + \mu)}$$

The derivatives are

$$K_\theta^\cdot = (\tfrac{4}{3} \times 1.2)\,\left(\frac{\lambda\mu_\theta^\cdot - \mu\lambda_\theta^\cdot}{(1.2\lambda + \mu)^2}\right)$$

$$K_\phi^\cdot = (\tfrac{4}{3} \times 1.2)\,\left(\frac{\lambda\mu_\phi^\cdot - \mu\lambda_\phi^\cdot}{(1.2\lambda + \mu)^2}\right)$$

$$K_\theta = (\tfrac{4}{3} \times 1.2)\,\left(\frac{\lambda\mu_\theta - \mu\lambda_\theta}{(1.2\lambda + \mu)^2}\right) \qquad (4)$$

$$= 0.0$$

$$K_\phi = (\tfrac{4}{3} \times 1.2)\,\left(\frac{\lambda\mu_\phi - \mu\lambda_\phi}{(1.2\lambda + \mu)^2}\right)$$

Equation 4.1.17 for the pitching moment M gives

$$M = Y_M\,(a_o \mu t_3 + \lambda_{o1}\, K t_4) \qquad (5)$$

The derivatives are

$$M_\theta^\cdot = Y_M\,(a_o t_3 \mu_\theta^\cdot + \lambda_{o1_\theta^\cdot}\, K t_4 + \lambda_{o1}\, K_\theta^\cdot t_4)$$

$$M_\phi^\cdot = Y_M\,(a_o t_3 \mu_\phi^\cdot + t_4(\lambda_{o1_\phi^\cdot} K + \lambda_{o1}\, K_\phi^\cdot)$$

$$M_\theta = Y_M\,(a_o t_3 \mu_\theta + t_4(\lambda_{o1_\theta} K + \lambda_{o1}\, K_\theta) \qquad (6)$$

$$M_\phi = Y_M\,(a_o t_3 \mu_\phi + t_4(\lambda_{o1_\phi} K + \lambda_{o1}\, K_\phi)$$

The control moment is

$$C_M = Y_M \left(A\left(t_4 + \tfrac{1}{4}\mu^2 t_2\right)\right)$$

The derivations are

$$\begin{aligned}
C_{M_\theta^\bullet} &= Y_M \left(A_\theta^\bullet\left(t_4 + \tfrac{1}{4}\mu^2 t_2\right) + \tfrac{1}{2}At_2\mu\,\mu_\theta^\bullet\right) \\
C_{M_\phi^\bullet} &= Y_M \left(A_\phi^\bullet\left(t_4 + \tfrac{1}{4}\mu^2 t_2\right) + \tfrac{1}{2}At_2\mu\,\mu_\phi^\bullet\right) \\
C_{M_\theta} &= Y_M \left(A_\theta\left(t_4 + \tfrac{1}{4}\mu^2 t_2\right) + \tfrac{1}{2}At_2\mu\,\mu_\theta\right) \\
C_{M_\phi} &= Y_M \left(A_\phi\left(t_4 + \tfrac{1}{4}\mu^2 t_2\right) + \tfrac{1}{2}At_2\mu\,\mu_\phi\right)
\end{aligned} \tag{7}$$

The H-force is

$$H = Y\left((H)_{induced} + (H)_{profile}\right)$$

$$= Y\left(\left(\tfrac{1}{2}\mu\lambda\theta t_1 - \tfrac{1}{2}t_2\,\lambda B + \tfrac{1}{2}a_o A t_3 + \tfrac{1}{2}a_o^2\mu\, t_2 + \tfrac{1}{2}a_o K\lambda t_3\right) + \mu\left(\frac{t_2\,\delta}{a}\right)\right)$$

The derivatives are

$$H_\theta^\bullet = Y\left(\left(\left(\frac{t_2\,\delta}{a}\right) + \tfrac{1}{2}\lambda\theta_c t_1 + \tfrac{1}{2}a_o^2 t_2\right)\mu_\theta^\bullet + \left(\tfrac{1}{2}\mu\theta t_1 - \tfrac{1}{2}t_2 B + \tfrac{1}{2}a_o K t_3\right)\right.$$

$$\lambda_\theta^\bullet + \left(-\tfrac{1}{2}t_2\,\lambda\right) B_\theta^\bullet + \tfrac{1}{2}a_o t_3 A_\theta^\bullet$$

$$\left. + \tfrac{1}{2}a_o\lambda\, t_3 K_\theta^\bullet\right) \tag{8}$$

Similar expressions for $H_{\dot{\phi}}$, H_{θ} and H_{ϕ} can be written,

$$H_{\dot{\phi}} = Y\left(\left(\frac{t_2\,\delta}{a} + \tfrac{1}{2}\lambda\theta t_1 + \tfrac{1}{2}a_o^2 t_2\right)\mu_{\dot{\phi}} + \left(\tfrac{1}{2}\mu\theta t_1 - \tfrac{1}{2}t_2 B + \tfrac{1}{2}a_o K t_3\right)\lambda_{\dot{\phi}} \right.$$

$$\left. + \left(-\tfrac{1}{2}t_2\,\lambda\right) B_{\dot{\phi}} + \tfrac{1}{2}a_o t_3\, A_{\dot{\phi}} + \tfrac{1}{2}a_o\,\lambda t_3 K_{\dot{\phi}} \right)$$

$$H_{\theta} = Y\left(\left(\frac{t_2\,\delta}{a} + \tfrac{1}{2}\lambda\theta t_1 + \tfrac{1}{2}a_o^2 t_2\right)\mu_{\theta} + \left(\tfrac{1}{2}\mu\theta t_1 - \tfrac{1}{2}t_2 B + \tfrac{1}{2}a_o K t_3\right)\lambda_{\theta} \right.$$

$$\left. + \left(-\tfrac{1}{2}t_2\,\lambda\right) B_{\theta} + \tfrac{1}{2}a_o t_3\, A_{\theta} + \tfrac{1}{2}a_o\lambda t_3\, K_{\theta} \right)$$

$$H_{\phi} = Y\left(\left(\frac{t_2\,\delta}{a} + \tfrac{1}{2}\lambda\theta t_1 + \tfrac{1}{2}a_o^2 t_2\right)\mu_{\theta} + \left(\tfrac{1}{2}\mu\theta t_1 - \tfrac{1}{2}t_2 B + \tfrac{1}{2}a_o K t_3\right)\lambda_{\phi} \right.$$

$$\left. + \left(-\tfrac{1}{2}t_2\,\lambda\right) B_{\phi} + \tfrac{1}{2}a_o t_3\, A_{\phi} + \tfrac{1}{2}a_o\, t_3\, K_{\phi} \right)$$

The aerodynamic drag and its derivatives can be approximated by

$$\begin{aligned} D &= \text{Constant}\quad V^2 \cos^2\alpha = \text{Constant}\quad \mu^2 \\ D_{\dot{\theta}} &= \text{Constant}\quad \mu_{\dot{\theta}} \\ D_{\dot{\phi}} &= \text{Constant}\quad \mu_{\dot{\phi}} \\ D_{\theta} &= \text{Constant}\quad \mu_{\theta} \\ D_{\phi} &= \text{Constant}\quad \mu_{\phi} \end{aligned} \tag{9}$$

2.2 Aerodynamic Derivatives for Zero-Wind Condition

Aerodynamic derivatives for zero-wind condition are easily obtained by putting V = 0 (or $\mu = 0$) in Equations 1 to 9 of Appendix 2.1. One obtains

$$\mu_{\dot{\theta}} = -\frac{\ell_1}{\Omega R}$$

$$\mu_{\dot{\phi}} = -\frac{\ell_2 + \ell_3}{\Omega R} \qquad (1a)$$

$$\mu_{\phi} = 0$$

$$\mu_{\theta} = 0$$

$$\lambda_{o2} = \lambda_{o2\,\dot{\theta}} = \lambda_{o2\,\dot{\phi}} = \lambda_{o2\,\phi} = \lambda_{o2\,\theta} = 0 \qquad (2a)$$

$$\lambda_{o1\,\dot{\theta}} = \lambda_{o1\,\dot{\phi}} = \lambda_{o1\,\phi} = \lambda_{o1\,\theta} = 0 \qquad (3a)$$

$$K_{\dot{\theta}} = \frac{4}{3 \times 1.2} \frac{\mu_{\dot{\theta}}}{\lambda_{o1}}$$

$$K_{\dot{\phi}} = \frac{4}{3 \times 1.2} \frac{\mu_{\dot{\phi}}}{\lambda_{o1}} \qquad (4a)$$

$$K_{\theta} = K_{\phi} = 0$$

Pitch moment M

$$M_{\dot{\theta}} = Y_M \left(a_o t_3 \mu_{\dot{\theta}} + \frac{4}{1.2 \times 3} t_4 \mu_{\dot{\theta}}\right)$$

$$= Y_M \left(a_o t_3 + \frac{4}{1.2 \times 3} t_4\right) \mu_{\dot{\theta}}$$

$$= k_2 \mu \dot{\theta}$$

where $k_2 = Y_M \left(a_o t_3 + \frac{4}{3 \times 1.2} t_4\right)$

$\simeq 800$

$$M_\phi^\bullet = k_2 \mu \dot{\phi}$$

$$M_\theta = M_\phi = 0 \qquad (6a)$$

Control moment C_M

$$C_{M\theta}^\bullet = Y_M \left(A_\theta^\bullet(t_4)\right)$$

$$= k_5 A_\theta^\bullet \qquad \text{where } k_5 = Y_M t_4 \simeq 600$$

$$C_{M\phi}^\bullet = k_5 A_\phi^\bullet \qquad (7a)$$

$$C_{M\phi} = k_5 A_\phi$$

$$C_{M\theta} = k_5 A_\theta$$

H-force

$$H_\theta^\bullet = Y \left(\left(\frac{t_2 \delta}{a} + \frac{1}{2}\lambda_{ol} \theta_c t_1 + \frac{1}{2}a_o^2 t_2 + \frac{1}{2}a_o \frac{4}{3 \times 1.2} t_3\right) \mu \dot{\theta} \right.$$

$$\left. + \frac{1}{2}a_o t_3 A_\theta^\bullet \right)$$

$$= k_1 \mu \dot{\theta} + k_3 A_\theta^\bullet$$

where $k_1 = Y \left(\frac{t_2 \delta}{a} + \frac{1}{2}\lambda_{ol} \theta_c t_1 + \frac{1}{2}a_o^2 t_2 + \frac{1}{2}a_o \frac{4}{1.2 \times 3} t_3\right)$

$\simeq 20$ to 50

and $k_3 = Y\left(\frac{1}{2}a_o t_3\right)$

$\simeq$ (20 to 50)

Similarly,

$$H_\phi^\bullet = k_1 \mu_\theta^\bullet + k_3 A_\phi^\bullet$$

$$H_\theta = k_3 A_\theta$$

$$H_\phi = k_3 A_\phi \qquad (8a)$$

Drag D

$$D_\theta^\bullet = D_\phi^\bullet = D_\phi = D_\theta = 0 \qquad (9a)$$

2.3 Coefficients of the Equations of Motion (V = 0)

$a_1 = m\ell_2$

$b_1 = -(D_\phi^\bullet + H_\phi^\bullet) = -(k_1 \mu_\phi^\bullet + k_3 A_\phi^\bullet)$

$c_1 = -W - P_o - D_\phi - H_\phi = -W - P_o - k_3 A_\phi$

$a_2 = m\ell_1$

$b_2 = -D_\theta^\bullet - H_\theta^\bullet = -(k \mu_\theta^\bullet + k_3 A_\theta^\bullet)$

$c_3 = P_o - H_\theta - D_\theta = P_o - k_3 A_\theta$

$a_3 = I$

$b_3 = M_\phi^\bullet + CM_\phi^\bullet - \ell_3 H_\phi^\bullet + \ell_4 D_\phi^\bullet$

$= (k_2 - \ell_3 k_1)\mu_\phi^\bullet + (k_5 - \ell_3 k_3) A_\phi^\bullet$

$$c_3 = M_\phi + CM_\phi - \ell_3 H_\phi + \ell_4 D_\phi$$

$$= \ell_2 P_o + (k_5 - \ell_3 k_3)\, A_\phi$$

$$a_4 = 0$$

$$b_4 = M_{\dot\theta} + CM_{\dot\theta} - \ell_3 H_{\dot\theta} + \ell_4 D_{\dot\theta}$$

$$= (k_2 - \ell_3 k_1)\mu_{\dot\theta} - (k_5 - \ell_3 k_3)\, A_{\dot\theta}$$

$$c_4 = -\ell_2 P_o + (k_5 - \ell_3 k_3)\, A_\theta$$

2.4 Evaluation of Coefficients of Stability Equation (4.3.10)

With the help of Equation 4.3.10 and the aerodynamic derivatives derived in Section 2.2 of the Appendix, one calculates the coefficients of the stability Equation 4.3.10 as follows

$$a = 1.0$$

$$b = \left(\frac{b_3}{a_3} - \frac{a_1 b_4}{a_2 a_3} + \frac{b_2}{a_2}\right)$$

$$= \frac{1}{I}\left((-k_2 - \ell_3 k_1)\mu_{\dot\phi} + (k_5 - \ell_3 k_3)\, A_{\dot\phi}\right) - \frac{\ell_2}{\ell_1 I}\left((-k_2 - \ell_3 k_1)\mu_{\dot\theta}\right.$$

$$\left. + (k_5 - \ell_3 k_3)\, A_{\dot\theta}\right) + \frac{1}{m\ell_1}\left(-k_1 \mu_{\dot\theta} - k_3 A_{\dot\theta}\right)$$

$$= \frac{1}{I\Omega R}\left(\frac{I}{m} k_1 + \ell_3 (k_2 + \ell_3 k_1)\right) + \left(\frac{k_5 - \ell_3 k_3}{I}\, A_{\dot\theta}\right.$$

$$\left. - \left(\frac{\ell_2}{I\ell_1}(k_5 - \ell_3 k_3) + \frac{k_3}{m\ell_1}\right) A_{\dot\theta}\right)$$

$$c = + \frac{1}{a_2 a_3}(b_2 b_3 - b_1 b_4) + \frac{c_3}{a_3} + \frac{c_2}{a_2} - \frac{a_1}{a_2}\frac{c_4}{a_3}$$

$$= \frac{1}{Im\ell_1}\Big(- (k_1 \mu_\theta^{\cdot} + k_3 A_\theta^{\cdot})\big((-k_2 - \ell_3 k_1)\mu_\phi^{\cdot} + (k_5 - \ell_3 k_3) A_\phi^{\cdot}\big)$$

$$+ (k_1 \mu_\phi^{\cdot} + k_3 A_\phi^{\cdot})(- k_2 - \ell_3 k_1)\mu_\theta^{\cdot} + (k_5 - \ell_3 k_3) A_\theta^{\cdot})\Big)$$

$$+ \frac{\ell_2 P_o}{I} + \frac{k_5 - \ell_3 k_3}{I} A_\phi + \frac{P_o - k_3 A_\theta}{m\ell_1} - \frac{\ell_2}{\ell_1 I}(- \ell_2 P_o + (k_5 - \ell_3 k_3) A_\theta)$$

$$= P_o\left(\frac{\ell_2}{I} + \frac{1}{m\ell_1} + \frac{\ell_2^2}{\ell_1 I}\right) + \frac{A_\phi^{\cdot}}{Im\Omega R}(k_1 (k_5 - \ell_3 k_3) + k_3(k_2 + \ell_3 k_1))$$

$$+ \frac{A_\theta^{\cdot}(\ell_2+\ell_3)}{Im\Omega R\ \ell_1}(- k_3 (k_2 + \ell_3 k_1) - k_1(k_5 - \ell_3 k_1))$$

$$+ \frac{k_5 - \ell_3 k_3}{I} A_\phi + A_\theta\left(\frac{-k_3}{m\ell_1} - \frac{\ell_2}{\ell_1 I}(k_5 - \ell_3 k_3)\right)$$

$$= P_o\left(\frac{\ell_2}{I} + \frac{1}{m\ell_1} + \frac{\ell_2^2}{\ell_1 I}\right) + \frac{1}{Im\Omega R}(k_1(k_5 - \ell_3 k_3) + k_3(k_2 + \ell_3 k_1))$$

$$(A_\phi^{\cdot} - \frac{\ell_2 + \ell_3}{\ell_1} A_\theta^{\cdot}) + \frac{k_5 - \ell_3 k_3}{I} A_\phi$$

$$- \left(\frac{k_3}{m\ell_1} + \frac{\ell_2}{\ell_1 I}(k_5 - \ell_3 k_3)\right) A_\theta$$

$$d = \frac{1}{a_2 a_3}(b_2 c_3 + b_3 c_2 - b_4 c_1 - b_1 c_4)$$

$$= \frac{1}{m\ell_1 I}\Big(- (k_1 \mu_\theta^{\cdot} + k_3 A_\theta^{\cdot})(\ell_2 P_o + (k_5 - \ell_3 k_3) A_\phi) + \big((- k_2 - \ell_3 k_1)\mu_\phi^{\cdot}$$

$$+ (k_5 - \ell_3 k_3) A_\phi^{\cdot}\big)(P_o - k_3 A_\theta) + (W + P_o + k_3 A_\phi)$$

$$\big((- k_2 - \ell_3 k_1)\mu_\theta^{\cdot} + (k_5 - \ell_3 k_3) A_\theta^{\cdot}\big) + (k_1 \mu_\phi^{\cdot} + k_3 A_\phi^{\cdot})$$

$$(-\ell_2 P_o + (k_5 - \ell_3 k_3) A_\theta))$$

$$= \frac{1}{mI\ell_1}(-\ell_2 P_o k_1 \mu_\theta^{\cdot} - P_o(k_2 + \ell_3 k_1)\mu_\phi^{\cdot} - (W + P_o)(k_2 + \ell_3 k_1)\mu_\theta^{\cdot}$$

$$- \ell_2 P_o k_1 \mu_\phi^{\cdot})$$

$$+ \frac{1}{mI\ell_1}(P_o(A_\phi^{\cdot} + A_\theta^{\cdot})((k_5 - \ell_3 k_3) - \ell_2 k_3) + W(k_5 - \ell_3 k_3) A_\theta^{\cdot})$$

$$+ \frac{1}{Im\Omega R}(k_1(k_5 - \ell_3 k_3) + k_3(k_2 + \ell_3 k_1))(A_\phi - \frac{\ell_2 + \ell_3}{\ell_1} A_\theta)$$

$$= \frac{P_o}{mI\Omega R}(\ell_2 k_1 + \frac{(k_2 + \ell_3 k_1)(\ell_2 + \ell_3)}{\ell_1} + (k_2 + \ell_3 k_1) + \frac{\ell_2(\ell_2 + \ell_3)}{\ell_1} k_1$$

$$+ \frac{W}{P_o}(k_2 + \ell_3 k_1))$$

$$+ \frac{P_o}{mI\ell_1}(((k_5 - \ell_3 k_3) - \ell_2 k_3)(A_\theta^{\cdot} + A_\phi^{\cdot}) + \frac{W}{P_o}(k_5 - \ell_3 k_3) A_\theta^{\cdot})$$

$$+ \frac{1}{Im\ R}(k_1(k_5 - \ell_3 k_3) + k_3(k_2 + \ell_3 k_1))(A_\phi - \frac{\ell_2 + \ell_3}{\ell_1} A_\theta)$$

$$e = -\frac{W P_o \ell_2}{Im\ell_1} + \frac{P_o}{Im\ell_1}((k_5 - \ell_3 k_3 - \ell_2 k_3)(A_\theta + A_\phi) + \frac{W}{P_o}(k_5 - \ell_3 k_3) A_\theta)$$